UNIVERSIDADE FEDERAL DE VIÇOSA

Cutaneous toxicity of the advanced glycation end products precursor methylglyoxal and the protective role of *Commiphora leptophloeos* extracts in an ex vivo skin model

Caroline Tomaz Massardi
Magister Scientiae

VIÇOSA - MINAS GERAIS
2025

CAROLINE TOMAZ MASSARDI

Cutaneous toxicity of the advanced glycation end products precursor methylglyoxal and the protective role of *Commiphora leptophloeos* extracts in an ex vivo skin model

Dissertation submitted to the Cell and Structural Biology Graduate Program of the Universidade Federal de Viçosa in partial fulfillment of the requirements for the degree of *Magister Scientiae*.

Adviser: Reggiani Vilela Goncalves

Co-advisers: Manoela M. dos S. Dias
Monica Morais Santos

VIÇOSA - MINAS GERAIS
2025

Ficha catalográfica elaborada pela Biblioteca Central da Universidade Federal de Viçosa - Campus Viçosa

T
M414c
2025

Massardi, Caroline Tomaz, 1997-
Cutaneous toxicity of the advanced glycation end products precursor methylglyoxal and the protective role of *Commiphora leptophloeos* extracts in an ex vivo skin model / Caroline Tomaz Massardi. – Viçosa, MG, 2025.
1 dissertação eletrônica (87 f.): il. (algumas color.).

Texto em inglês.
Orientador: Reggiani Vilela Gonçalves.
Dissertação (mestrado) - Universidade Federal de Viçosa, Departamento de Biologia Geral, 2025.
Inclui bibliografia.
DOI: https://doi.org/10.47328/ufvbbt.2025.571
Modo de acesso: World Wide Web.

1. Doenças inflamatórias da pele. 2. Estresse oxidativo. 3. *Commiphora leptophloeos*. I. Gonçalves, Reggiani Vilela, 1979-. II. Universidade Federal de Viçosa. Departamento de Biologia Geral. Programa de Pós-Graduação em Biologia Celular e Estrutural. III. Título.

CDD 22. ed. 573.539

Bibliotecário(a) responsável: Euzébio Luiz Pinto CRB-6/3317

CAROLINE TOMAZ MASSARDI

Cutaneous toxicity of the advanced glycation end products precursor methylglyoxal and the protective role of *Commiphora leptophloeos* extracts in an ex vivo skin model

Dissertation submitted to the Cell and Structural Biology Graduate Program of the Universidade Federal de Viçosa in partial fulfillment of the requirements for the degree of *Magister Scientiae*.

APPROVED: August 6, 2025.

Assent:

Caroline Tomaz Massardi
Author

Reggiani Vilela Goncalves
Adviser

Dedico este trabalho, com tudo o que ele significa, para todas as mulheres que vieram antes de mim e possibilitaram que hoje eu estivesse aqui e para todas aquelas que ainda virão.

ACKNOWLEDGMENTS

Agradeço aos meus pais, Ivair e Sandra, por nunca medirem esforços para me ajudar a chegar onde quero. Aos meus irmãos Natan e Gabriel, pelo companheirismo de todos os dias, aos quatro: amo vocês de sempre, para sempre, vocês sabem o quanto representam!

Agradeço também aos meus amigos da vida e principalmente aqueles que me acompanharam durante toda essa jornada, destacando Luísa, Filipe, Eduarda e Allan.

Agradeço a toda equipe do Laboratório de Patologia Experimental, por toda ajuda e apoio, principalmente à minha companheira de bancada Eduarda, Allan, Néia, Filipe e Manu.

Agradeço à minha orientadora Reggiani, pela oportunidade de fazer a pós graduação no LAPEX e por todo o aprendizado adquirido nesses anos desde a graduação.

Agradeço às minhas co-orientadoras, Mônica e Manoela por todo suporte, ensinamentos e acolhimento.

Por fim e não menos importante, agradeço à Universidade Federal de Viçosa, pela oportunidade de realizar a pós- graduação.

This work has been sponsored by the following Brazilian research agencies: Coordination for the Improvement of Higher Education Personnel (CAPES; Financing code 001), Minas Gerais State Foundation for Research Aid (FAPEMIG) and National Council of Scientific and Technological Development (CNPq).

ABSTRACT

MASSARDI, Caroline Tomaz, M.Sc., Universidade Federal de Viçosa, August, 2025. **Cutaneous toxicity of the advanced glycation end products precursor methylglyoxal and the protective role of *Commiphora leptophloeos* extracts in an ex vivo skin model**. Adviser: Reggiani Vilela Goncalves. Co-advisers: Manoela Maciel dos Santos Dias and Monica Morais Santos.

The skin represents the body's first barrier against the external environment and is therefore constantly exposed to potentially harmful agents such as pollution, ultraviolet radiation, microorganisms, and even physical damage (Woodby et al., 2020). Maintaining skin homeostasis is essential to support the overall homeostasis of the organism (Dehkordi et al., 2019). This organ, the largest in the human body, is composed of two principal layers: the epidermis (outer) and the dermis (inner). The epidermis can be further subdivided into five strata, arranged from the innermost to the outermost: basal layer, spinous layer, granular layer, lucid layer (present only in thick skin), and corneal layer. The epidermal cells are predominantly epithelial cells, or keratinocytes, except in the outermost layer, where they are referred to as corneocytes. This stratification reflects the progressive differentiation of keratinocytes until they reach the stratum corneum. The basal layer is characterized by intense mitotic activity, giving rise to new keratinocytes. The granular layer contains keratinocytes rich in keratohyalin granules, which are essential for maintaining the structural integrity, resilience, and hydration of the skin. The stratum corneum, composed of corneocytes, is distinguished by the absence of nuclei and organelles, consisting instead of keratin-rich cells. The dermis is composed of connective tissue and contains nerve endings and blood vessels that provide nutrition and oxygen to the overlying epithelial cells. It also harbors skin appendages, including glands and follicles (Junqueira & Carneiro, 2022). It is now well established that inflammation and oxidative stress are interdependent processes, mutually reinforcing each other. Reactive species generated by oxidative stress trigger inflammatory responses, while inflammatory mediators can exacerbate oxidative stress. This feedback loop is referred to as oxi-inflammation (Farris et al., 2022; Valacchi et al., 2018). Oxi-inflammation promotes the formation of Advanced Glycation End-products (AGEs) (Sruthi & Raghu, 2021). AGEs are molecules generated through non-enzymatic reactions in which glucose reacts with proteins, lipids, or nucleic acids—a process known as glycation (Singh, 2001). Glycation is harmful because it occurs spontaneously and uncontrollably, altering the structure of biomolecules and leading to multiple cellular impairments,

including protein dysfunction, apoptosis, cellular senescence, mitochondrial disturbances, inflammation, and oxidative stress (Ansari & Dash, 2012). Among the compounds capable of inducing oxidative stress and inflammatory processes, methylglyoxal (MGO) is of particular importance (Desai et al., 2010). MGO is an endogenous aldehyde present in all mammals, produced as a byproduct of glucose metabolism (Thornalley, 1996). Under physiological conditions, MGO is detoxified by the glyoxalase system, an enzymatic pathway responsible for its clearance. However, when cellular homeostasis is disrupted and this pathway becomes impaired, MGO can accumulate (Polykretis et al., 2020). The danger lies in its high reactivity, as MGO readily interacts with proteins, lipids, and nucleic acids, acting as a precursor of AGEs (Lo et al., 1994; Rabbani & Thornalley, 2008). For this reason, MGO is frequently employed in laboratory models to induce cellular stress. For example, in order to evaluate the efficacy of antioxidant compounds, it is first necessary to induce oxidative stress in cells or tissues. Once stressed, the application of candidate compounds allows the assessment of their potential antioxidant and anti-inflammatory effects. In recent years, the search for natural compounds capable of modulating inflammation and oxidative stress has gained increasing attention. One such plant used in Brazilian folk medicine is Commiphora leptophloeos, commonly known as Imburana. This species is endemic to the Caatinga biome in northeastern Brazil (De Melo Alcântara et al., 2023). Extracts prepared from its leaves and bark can be tested for biological activity in models of inflamed or stressed tissues (Dantas-Medeiros et al., 2021). To reduce or replace the use of animal models or direct human subjects in clinical testing, ex vivo approaches have emerged as valuable alternatives. These involve the study of tissues removed from the body and maintained under controlled laboratory conditions while preserving much of their original physiological properties (Neil et al., 2022). In this study, ex vivo experiments were conducted using skin explants obtained from patients undergoing elective plastic surgery in Viçosa. The objective of this dissertation was twofold: first, to investigate the effects of methylglyoxal on skin tissue and establish a working concentration for laboratory use; second, to employ this concentration as a stress-inducing agent in order to evaluate the anti-inflammatory and antioxidant properties of Imburana leaf and bark extracts in an ex vivo skin model. Accordingly, the dissertation is divided into two chapters corresponding to separate articles. The first presents the experiments and results regarding methylglyoxal as a stress-inducing agent, while the second reports the effects of Imburana extracts on inflamed and stressed skin tissue using the concentration established in the first study. The articles are presented in different formats due to the

publication requirements of the journals to which they were submitted.

Keywords: oxiinflammation; skin; ex vivo; methylglyoxal; *Commiphora leptophloeos*

RESUMO

MASSARDI, Caroline Tomaz, M.Sc., Universidade Federal de Viçosa, agosto de 2025. **Toxicidade cutânea do precursor dos produtos finais de glicação avançada metilglioxal e o papel protetor dos extratos de *Commiphora leptophloeos* em um modelo de pele ex vivo**. Orientadora: Reggiani Vilela Goncalves. Coorientadores: Manoela Maciel dos Santos Dias e Monica Morais Santos.

A pele representa a primeira barreira do corpo contra o ambiente externo e, portanto, está constantemente exposta a agentes potencialmente nocivos, como poluição, radiação ultravioleta, microrganismos e até mesmo danos físicos (Woodby et al., 2020). Manter a homeostase da pele é essencial para sustentar a homeostase geral do organismo (Dehkordi et al., 2019). Esse órgão, o maior do corpo humano, é composto por duas camadas principais: a epiderme (externa) e a derme (interna). A epiderme pode ser subdividida em cinco estratos, organizados do mais interno ao mais externo: camada basal, camada espinhosa, camada granulosa, camada lúcida (presente apenas em pele espessa) e camada córnea. As células epidérmicas são predominantemente células epiteliais, ou queratinócitos, exceto na camada mais externa, onde passam a ser chamadas de corneócitos. Essa estratificação reflete a diferenciação progressiva dos queratinócitos até alcançarem o estrato córneo. A camada basal é caracterizada por intensa atividade mitótica, dando origem a novos queratinócitos. A camada granulosa contém queratinócitos ricos em grânulos de querato-hialina, essenciais para a manutenção da integridade estrutural, resiliência e hidratação da pele. O estrato córneo, composto por corneócitos, distingue-se pela ausência de núcleos e organelas, consistindo em células ricas em queratina. A derme é composta por tecido conjuntivo e contém terminações nervosas e vasos sanguíneos que fornecem nutrição e oxigênio às células epiteliais sobrejacentes. Também abriga anexos cutâneos, incluindo glândulas e folículos (Junqueira & Carneiro, 2022). Está bem estabelecido que inflamação e estresse oxidativo são processos interdependentes, que se reforçam mutuamente. Espécies reativas geradas pelo estresse oxidativo desencadeiam respostas inflamatórias, enquanto mediadores inflamatórios podem exacerbar o estresse oxidativo. Esse ciclo de retroalimentação é denominado oxi-inflamação (Farris et al., 2022; Valacchi et al., 2018). A oxi-inflamação promove a formação de Produtos Finais de Glicação Avançada (AGEs) (Sruthi & Raghu, 2021). Os AGEs são moléculas geradas por meio de reações não enzimáticas nas quais a glicose reage com proteínas, lipídios ou ácidos nucleicos — processo conhecido como glicação (Singh, 2001). A glicação é prejudicial porque ocorre de forma espontânea e incontrolável,

alterando a estrutura das biomoléculas e levando a múltiplos comprometimentos celulares, incluindo disfunção proteica, apoptose, senescência celular, distúrbios mitocondriais, inflamação e estresse oxidativo (Ansari & Dash, 2012). Entre os compostos capazes de induzir estresse oxidativo e processos inflamatórios, o metilglioxal (MGO) é de particular importância (Desai et al., 2010). O MGO é um aldeído endógeno presente em todos os mamíferos, produzido como subproduto do metabolismo da glicose (Thornalley, 1996). Em condições fisiológicas, o MGO é detoxificado pelo sistema glioxalase, uma via enzimática responsável pela sua depuração. No entanto, quando a homeostase celular é comprometida e essa via se torna deficiente, o MGO pode se acumular (Polykretis et al., 2020). O perigo reside em sua alta reatividade, já que o MGO interage facilmente com proteínas, lipídios e ácidos nucleicos, atuando como precursor dos AGEs (Lo et al., 1994; Rabbani & Thornalley, 2008). Por esse motivo, o MGO é frequentemente empregado em modelos laboratoriais para induzir estresse celular. Por exemplo, para avaliar a eficácia de compostos antioxidantes, é necessário primeiro induzir estresse oxidativo em células ou tecidos. Uma vez estressados, a aplicação dos compostos candidatos permite avaliar seus potenciais efeitos antioxidantes e anti-inflamatórios. Nos últimos anos, a busca por compostos naturais capazes de modular inflamação e estresse oxidativo tem recebido crescente atenção. Uma dessas plantas utilizadas na medicina popular brasileira é a *Commiphora leptophloeos*, conhecida popularmente como Imburana. Essa espécie é endêmica do bioma Caatinga, no nordeste do Brasil (De Melo Alcântara et al., 2023). Extratos preparados a partir de suas folhas e cascas podem ser testados quanto à atividade biológica em modelos de tecidos inflamados ou estressados (Dantas-Medeiros et al., 2021). Para reduzir ou substituir o uso de modelos animais ou de voluntários humanos em testes clínicos, abordagens ex vivo surgiram como alternativas valiosas. Essas envolvem o estudo de tecidos removidos do corpo e mantidos sob condições laboratoriais controladas, preservando grande parte de suas propriedades fisiológicas originais (Neil et al., 2022). Neste estudo, experimentos ex vivo foram conduzidos utilizando explantes de pele obtidos de pacientes submetidos a cirurgias plásticas eletivas em Viçosa. O objetivo desta dissertação foi duplo: primeiro, investigar os efeitos do metilglioxal sobre o tecido cutâneo e estabelecer uma concentração de trabalho para uso laboratorial; segundo, empregar essa concentração como agente indutor de estresse, a fim de avaliar as propriedades anti-inflamatórias e antioxidantes dos extratos de folhas e cascas de Imburana em um modelo ex vivo de pele. Assim, a dissertação está dividida em dois capítulos correspondentes a artigos distintos. O primeiro apresenta os experimentos e resultados referentes ao

metilglioxal como agente indutor de estresse, enquanto o segundo relata os efeitos dos extratos de Imburana em tecido cutâneo inflamado e estressado, utilizando a concentração estabelecida no primeiro estudo. Os artigos são apresentados em formatos diferentes devido às exigências de publicação dos periódicos aos quais foram submetidos.

Palavras-chave: oxi-inflamação; pele; ex vivo; metilglioxal; *Commiphora leptophloeos*

Sumário

1. General Introduction

The skin represents the body's first barrier against the external environment and is therefore constantly exposed to potentially harmful agents such as pollution, ultraviolet radiation, microorganisms, and even physical damage (Woodby et al., 2020). Maintaining skin homeostasis is essential to support the overall homeostasis of the organism (Dehkordi et al., 2019). This organ, the largest in the human body, is composed of two principal layers: the epidermis (outer) and the dermis (inner).

The epidermis can be further subdivided into five strata, arranged from the innermost to the outermost: basal layer, spinous layer, granular layer, lucid layer (present only in thick skin), and corneal layer. The epidermal cells are predominantly epithelial cells, or keratinocytes, except in the outermost layer, where they are referred to as corneocytes. This stratification reflects the progressive differentiation of keratinocytes until they reach the stratum corneum. The basal layer is characterized by intense mitotic activity, giving rise to new keratinocytes. The granular layer contains keratinocytes rich in keratohyalin granules, which are essential for maintaining the structural integrity, resilience, and hydration of the skin. The stratum corneum, composed of corneocytes, is distinguished by the absence of nuclei and organelles, consisting instead of keratin-rich cells.

The dermis is composed of connective tissue and contains nerve endings and blood vessels that provide nutrition and oxygen to the overlying epithelial cells. It also harbors skin appendages, including glands and follicles (Junqueira & Carneiro, 2022).

It is now well established that inflammation and oxidative stress are interdependent processes, mutually reinforcing each other. Reactive species generated by oxidative stress trigger inflammatory responses, while inflammatory mediators can exacerbate oxidative stress. This feedback loop is referred to as oxi-inflammation (Farris et al., 2022; Valacchi et al., 2018).

Oxi-inflammation promotes the formation of Advanced Glycation End-products (AGEs) (Sruthi & Raghu, 2021). AGEs are molecules generated through non-enzymatic reactions in which glucose reacts with proteins, lipids, or nucleic acids—a process known as glycation (Singh, 2001). Glycation is harmful because it occurs spontaneously and uncontrollably, altering the structure of biomolecules and leading to multiple cellular impairments, including

protein dysfunction, apoptosis, cellular senescence, mitochondrial disturbances, inflammation, and oxidative stress (Ansari & Dash, 2012).

Among the compounds capable of inducing oxidative stress and inflammatory processes, methylglyoxal (MGO) is of particular importance (Desai et al., 2010). MGO is an endogenous aldehyde present in all mammals, produced as a byproduct of glucose metabolism (Thornalley, 1996). Under physiological conditions, MGO is detoxified by the glyoxalase system, an enzymatic pathway responsible for its clearance. However, when cellular homeostasis is disrupted and this pathway becomes impaired, MGO can accumulate (Polykretis et al., 2020). The danger lies in its high reactivity, as MGO readily interacts with proteins, lipids, and nucleic acids, acting as a precursor of AGEs (Lo et al., 1994; Rabbani & Thornalley, 2008). For this reason, MGO is frequently employed in laboratory models to induce cellular stress. For example, in order to evaluate the efficacy of antioxidant compounds, it is first necessary to induce oxidative stress in cells or tissues. Once stressed, the application of candidate compounds allows the assessment of their potential antioxidant and anti-inflammatory effects.

In recent years, the search for natural compounds capable of modulating inflammation and oxidative stress has gained increasing attention. One such plant used in Brazilian folk medicine is *Commiphora leptophloeos,* commonly known as *Imburana*. This species is endemic to the Caatinga biome in northeastern Brazil (De Melo Alcântara et al., 2023). Extracts prepared from its leaves and bark can be tested for biological activity in models of inflamed or stressed tissues (Dantas-Medeiros et al., 2021).

To reduce or replace the use of animal models or direct human subjects in clinical testing, *ex vivo* approaches have emerged as valuable alternatives. These involve the study of tissues removed from the body and maintained under controlled laboratory conditions while preserving much of their original physiological properties (Neil et al., 2022). In this study, ex vivo experiments were conducted using skin explants obtained from patients undergoing elective plastic surgery in Viçosa.

The objective of this dissertation was twofold: first, to investigate the effects of methylglyoxal on skin tissue and establish a working concentration for laboratory use; second, to employ this concentration as a stress-inducing agent in order to evaluate the anti-inflammatory and antioxidant properties of *Imburana* leaf and bark extracts in an ex vivo skin model. Accordingly, the dissertation is divided into two chapters corresponding to separate articles.

The first presents the experiments and results regarding methylglyoxal as a stress-inducing agent, while the second reports the effects of *Imburana* extracts on inflamed and stressed skin tissue using the concentration established in the first study. The articles are presented in different formats due to the publication requirements of the journals to which they were submitted.

2. References

Ansari, Nadeem A.; Dash, Debabrata. Amadori glycated proteins: role in production of autoantibodies in diabetes mellitus and effect of inhibitors on non-enzymatic glycation. **Aging and disease**, v. 4, n. 1, p. 50, 2012.

Dantas-Medeiros, Renato et al. Mass spectrometry characterization of Commiphora leptophloeos leaf extract and preclinical evaluation of toxicity and anti-inflammatory potential effect. **Journal of Ethnopharmacology**, v. 264, p. 113229, 2021.

De Melo Alcântara, Lucas Felipe et al. Toxicological safety, antioxidant activity and phytochemical characterization of leaf and bark aqueous extracts of Commiphora leptophloeos (Mart.) JB Gillett. **Journal of Toxicology and Environmental Health**, Part A, v. 86, n. 16, p. 557-574, 2023.

Desai, Kaushik M. et al. Oxidative stress and aging: is methylglyoxal the hidden enemy? **Canadian journal of physiology and pharmacology**, v. 88, n. 3, p. 273-284, 2010.

Farris, Patricia K.; Valacchi, Giuseppe. Ultraviolet light protection: is it really enough?. **Antioxidants**, v. 11, n. 8, p. 1484, 2022.

JUNQUEIRA, Luiz Carlos Uchôa; CARNEIRO, José. **Histologia básica: texto e atlas.** 14. ed. Rio de Janeiro: Guanabara Koogan, 2022.

Lo, T. W. et al. Binding and modification of proteins by methylglyoxal under physiological conditions. A kinetic and mechanistic study with N alpha-acetylarginine, N alpha-acetylcysteine, and N alpha-acetyllysine, and bovine serum albumin. **Journal of Biological Chemistry**, v. 269, n. 51, p. 32299-32305, 1994.

Neil, MS Jessica E. et al. A new ex vivo skin model for mechanistic understanding of putative anti-inflammatory topical therapeutics. **International Journal of Pharmaceutics**, v. 617, p. 121610, 2022.

Rabbani, Naila; Thornalley, Paul J. Dicarbonyls linked to damage in the powerhouse: glycation of mitochondrial proteins and oxidative stress. 2008.

Singh, R. B. A. M. et al. Advanced glycation end-products: a review. **Diabetologia**, v. 44, p. 129-146, 2001.

Sruthi, C. R.; Raghu, K. G. Advanced glycation end products and their adverse effects: the role of autophagy. **Journal of Biochemical and Molecular Toxicology**, v. 35, n. 4, p. e22710, 2021.

Thornalley, Paul J. Pharmacology of methylglyoxal: formation, modification of proteins and nucleic acids, and enzymatic detoxification-a role in pathogenesis and antiproliferative chemotherapy. **General Pharmacology: The Vascular System**, v. 27, n. 4, p. 565-573, 1996.

Valacchi, G. et al. Ox-Inflammation: from subclinical condition to pathological biomarker. **Front. Physiol.** 9: e858. 2018.

Woodby, Brittany et al. Skin health from the inside out. **Annual review of food science and technology**, v. 11, n. 1, p. 235-254, 2020.

Yang, Chun-tao et al. A novel controllable hydrogen sulfide-releasing molecule protects human skin keratinocytes against methylglyoxal-induced injury and dysfunction. **Cellular Physiology and Biochemistry**, v. 34, n. 4, p. 1304-1317, 2014.

1. Cutaneous toxicity of the Advanced Glycation End Products precursor methylglyoxal

Caroline Tomaz Massardi[1], Eduarda Pires Costa[1], Mônica Morais Santos[2], Manoela Maciel dos Santos Dias[2], Rosinea Aparecida de Paula[2], Carlos Eduardo Soares Gazzinelli Cruz[3], Giuseppe Valacchi[4], Reggiani Vilela Gonçalves*[2,4]

[1] Department of General Biology, Federal University of Viçosa, Peter Henry Rolfs Ave, s/n, University Campus, Viçosa, MG, 36570-900, Brazil; caroline.massardi@ufv.br; eduarda.costa@ufv.br

[2] Department of Animal Biology, Federal University of Viçosa, Peter Henry Rolfs Ave, s/n, University Campus, Viçosa, MG, 36570-900, Brazil; monica.morais@ufv.br; manoela.santos@ufv.br; rosinea.paula@ufv.br; reggiani.goncalves@ufv.br

[3] Department of Medicine and Nursing, Federal University of Viçosa, Peter Henry Rolfs Ave, s/n, University Campus – Viçosa, MG 36570-900, Brazil; carlos.gazzinelli@ufv.br

[4] Department of Animal Sciences, Plants for Human Health Institute, North Carolina State University, Kannapolis, NC 28081, USA. gvalacc@ncsu.edu; rvilela@ncsu.edu

*Corresponding author: Reggiani Vilela Gonçalves; rvilela@ncsu.edu / reggiani.goncalves@ufv.br

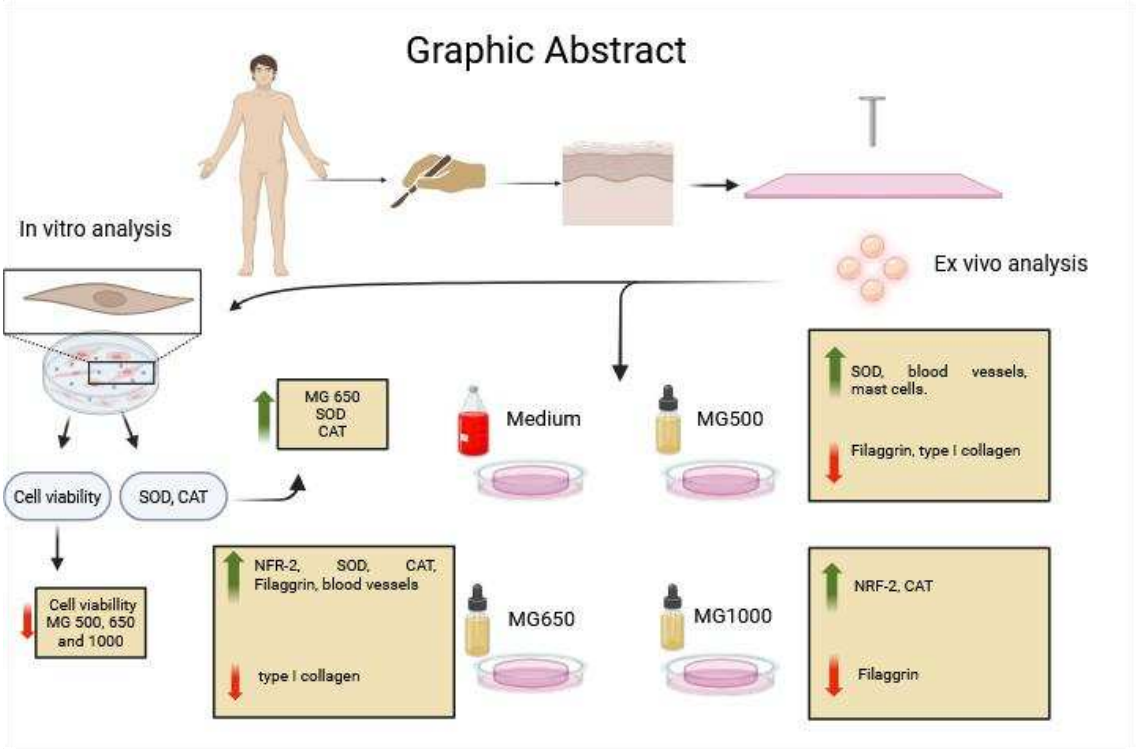

Abstract

The skin is the largest sensory organ of the human body and serves as the primary interface with the external environment, rendering it susceptible to various environmental stressors, including pollution, ultraviolet (UV) radiation, and other physical, chemical, and/or biological agents. These harmful factors can trigger biochemical alteration within the tissue, leading to inflammation and oxidative stress through excessive generation of reactive oxygen species (ROS). This study aimed to evaluate the effects of different concentrations of methylglyoxal (MG), a precursor of advanced glycation end products **(**AGEs), as a cellular stressor using *in vitro* and *ex vivo* models to understand the skin dose response in term of OxInflammatory process. Therefore, three MG concentrations (500, 650, and 1000 µM) were assessed and compared to the control group. The results showed that exposure to 650 µM MG led to a significant increase in the activities of key antioxidant enzymes such as Catalase (CAT) and superoxide dismutase (SOD) levels. Additionally, MG was able to alter the levels of filaggrin, 4HNE and 8-OHDG levels as assessed by immunohistochemical analyses. The morphological changes were observed by the decrease in collagen I fibers, and mast cells without promoting a change in blood vessels and epidermis thickness. In gene expression, we observe an increase in NFR-2 expression.

Keywords: AGEs; Oxidative stress; OxInflammation; Filaggrin; 4HNE.

1.1. Introduction

Skin is the largest organ of the human body and serves as the primary barrier in contact with the external environment, being vulnerable to pollution, ultraviolet (UV) radiation, and other physical, chemical, and/or biological stressors.[1] These different harmful agents can promote biochemical changes within the tissue, causing inflammation and oxidative stress through excessive generation of reactive oxygen species (ROS).[2,3] The process in which there is an interaction between oxidative stress and inflammation is known as OxInflammation,[4,5] and can lead to the formation of Advanced Glycation End Products (AGEs).[6]

Advanced Glycation End Products (AGEs) constitute a heterogeneous group of molecules derived from a non-enzymatic process known as glycation, wherein glucose molecules react with free amino groups of proteins and lipids. This reaction proceeds through a series of chemical steps, initially leading to the formation of Schiff bases and subsequently Amadori products, which eventually result in the generation of AGEs.[7] These AGEs exert multiple detrimental effects on cellular function, including the induction of apoptosis, inflammation, mitochondrial dysfunction, oxidative stress, and protein malfunction.[6]

It is well established that various compounds can induce oxidative stress and, consequently, trigger inflammation in cells and tissues, with methylglyoxal (MG) being one such molecule.[8] MG is an endogenous aldehyde present in all mammals,[9] primarily formed as a byproduct of glucose metabolism, protein catabolism, and lipid peroxidation.[10] Due to its high reactivity, MG can exert cytotoxic effects if not adequately neutralized by the glyoxalase system, a key enzymatic pathway responsible for its detoxification.[11] The accumulation of MG can lead to mutagenicity and protein degradation due to its strong reactivity with proteins, lipids, and fatty acids.[12] Furthermore, MG interacts with mitochondria by binding to mitochondrial proteins and promoting the formation of AGEs, which, in turn, enhance superoxide production within the organelle.[13] These molecular alterations contribute to oxidative stress and are implicated in the pathogenesis of various diseases, including diabetes, cancer, and tissue aging.[14]

When the skin tissue is compromised by burns, wounds, chemical exposure, pollution, and others, a cascade of biochemical alterations is triggered, potentially disrupting skin homeostasis.[15] The initial response is the development of inflammation, activating cell migration and macrophages that will be responsible for the release of respiratory bursts.16 Free radicals and ROS can work as messengers to induce the release of inflammatory markers and cytokines involved in the OxInflammation process.[17] At low levels, ROS can play essential roles inside the cells, including cell survival, differentiation,[18] and modulating

wound healing and inflammatory process.[19] However, if there is an exacerbated levels in ROS, they can interact with membranes and lipids, leading to permanent and irreversible tissue damage.[20] This response is further modulated by the release of inflammatory mediators, which act as either inducers (pro- inflammatory mediators) or suppressors (anti-inflammatory mediators) in the regulation of the inflammatory process.[19]

There is a well-established consensus regarding the role of oxidative stress and subsequent inflammation in cellular and tissue responses following exposure to MG. However, the optimal concentrations of MG required to induce the OxInflammation process without triggering extensive cell death or irreversible tissue damage remain unclear. Furthermore, the key molecular mechanisms activated in response to this optimal MG concentration have yet to be fully elucidated. To date, no ex vivo studies using human skin biopsies have been conducted to investigate the molecular pathway activated and the primary morphological damage induced by exposure to an optimal MG concentration. The *ex vivo* model provides a more physiologically relevant representation of skin biochemistry and structural integrity, while also providing a non-invasive experimental approach.[21] Therefore, this study aimed to evaluate the effects of varying concentrations of MG (500, 650, and 1000 μM) using both *in vitro* models and human skin biopsies, with the objective of elucidating the specific impacts of each concentration on cutaneous tissue and establishing reference parameters for the application of MG in future *ex vivo* assays.

1.2. Materials and Methods

1.2.1. Ex Vivo Analyses Using Human Skin Biopsies

The skin biopsies used in this study were donated from elective abdominoplasty procedures performed in Viçosa, Minas Gerais, Brazil. The collection of biological material and all experimental procedures were approved by the Ethics Committee on Research with Human Beings (CEP) of the Federal University of Viçosa (approval number 82329224.7.0000.5153). Upon arrival, human skin biopsies (12 mm) were processed by removing the subcutaneous fat with a scalpel, followed by washing in phosphate-buffered saline (PBS). The biopsies were then placed in six-well plates and cultured in Dulbecco's Modified Eagle Medium (DMEM) High Glucose (GIBCO, USA) supplemented with 1% Fetal Bovine Serum (FBS; GIBCO, USA), 1% liquid penicillin, and 2.5 μg/mL of amphotericin B. The samples were incubated for 24 hours (5% CO2, 37°C) for tissue

recovery.[22] Following the recovery period, the biopsies were treated for seven days with a DMEM High Glucose medium containing 500, 650, and 1000 µM of methylglyoxal. The experimental groups were designated as follows: CN (Control), MG500 (500 µM MG exposure), MG650 (650µM MG exposure), and MG1000 (1000µM MG exposure). Negative controls were maintained in DMEM medium without MG exposure. To ensure consistent exposure conditions, the culture medium in all MG-treated plates was replaced daily throughout the experiment.

1.2.2. Cell Culture

The fibroblasts used in the *in vitro* analyses were derived from primary cell isolated from the skin biopsies, following the protocol described by Valacchi et al. (2020)[23]. After obtaining the skin samples, as described in Section 2.1, tissue fragments were incubated in six-well plates containing 1.5 mL of low glucose DMEM supplemented with 20% Fetal Bovine Serum, 1% liquid penicillin, and 2.5 µg/mL of amphotericin B. The plates were maintained under standard cell culture conditions (5% CO_2, 37°C) to facilitate fibroblast migration from the tissue fragments to the culture plate. The culture medium was changed every 48 hours throughout the migration period. Once fibroblast migration resulted in more than 90% confluency, the remaining skin fragments were discarded, and the fibroblasts were transferred to new plates containing the same culture medium. Cell proliferation was repeated until sufficient fibroblasts were obtained for experimental assays.

1.2.3. Cell Viability

Fibroblasts were seeded in 96-well plates at a density of $2x10^4$ cells/well, using low glucose medium with 10% Fetal Bovine Serum, 1% liquid penicillin, and 2.5 µg/mL of amphotericin B (5% CO_2, 37°C) for 24 hours and exposed to different concentrations of methylglyoxal for 4 hours to determine the stress-inducing effect of MG. Cell viability was assessed using the 3-(4,5-dimethylthiazol-2-yl)-2,5-diphenyltetrazolium bromide (MTT) reduction method as described by Mu et al. (2014)[24]. This colorimetric assay is based on the reduction of the yellow tetrazolium salt to purple formazan crystals by metabolically active cells. The control group (100% growth) comprised cells cultured in a medium without MG exposure. To assess cell viability, 50 µL of supernatant was removed from each well, and an equal volume (50 µL) of MTT solution (0.5 mg/mL) was added. The cells were then

incubated at 37°C for 2 hours to allow for formazan crystal formation. Following incubation, the supernatant was carefully removed, and 100 µL of dimethyl sulfoxide (DMSO) was added to dissolve the formazan crystals. The absorbance was then measured at 570 nm, and the results were expressed as a percentage of absorbance relative to the control group.

1.2.4. Antioxidant Enzyme Activity

The primary fibroblasts were cultured at a density of 1×10^5 cells/well in a 96-well plate for 24 hours under standard conditions (5% CO_2, 37°C). The culture medium consisted of 199 medium with low glucose, supplemented with 20% Fetal Bovine Serum, 1% liquid penicillin, and 2.5 µg/mL of amphotericin B. Following the period, the cells were exposed to different MG concentrations (500, 650, 1000 µM) for 4 hours. Subsequently, the culture medium was discarded, and the cells were lysed using PBS containing 1% Triton X-100 to facilitate the assessment of catalase (CAT) and superoxide dismutase (SOD) enzymatic activities. The CAT activity, defined by the ability to cleave hydrogen peroxide into water and oxygen, was measured according to the methodology proposed by Aebi (1984)[25]. A 5 µL aliquot of the sample was transferred to the wells, followed by 100 µL of a 20 mM H_2O_2 solution. After 3 minutes of reaction, 150 µL of ammonium molybdate was added. A standard curve for H_2O_2 was prepared, ranging from 20 to 0.078 mM. The absorbance was measured at 374 nm. To assess SOD catalytic activity, 30 µL of the sample was mixed with 99 µL of phosphate buffer (0.2 M, pH 8.0), 6 µL of MTT (1.25 mM), and 15 µL of pyrogallol (100 µM) in a 96-well plate. The mixture was incubated at 40 ºC for 15 minutes. A standard control and a blank were prepared similarly but without the sample—using 129 µL and 144 µL of buffer, respectively. Pyrogallol was omitted from the blank. After incubation, the reaction was stopped by adding 150 µL of DMSO, and absorbance was recorded at 540 nm using a Thermo Scientific Multiskan™ GO plate reader.

1.2.5. Human biopsies

1.2.5.1. Antioxidant Enzymes Activity and Oxidative Stress Markers

After the seven-day exposure to MG, the fragments designated for oxidative stress analysis were immediately frozen in liquid nitrogen (-196°C) and stored in an ultrafreezer (-80°C) for further analysis. The samples were weighed and manually macerated in liquid nitrogen using a pestle and homogenized with EDTA buffer - phosphate buffer 0.2 mol/L, 1

mmol/L of ethylenediaminetetraacetic acid (pH 7.4). After homogenization, the samples were centrifuged at 15.000g for 10 minutes at 4°C. The supernatants were used to measure CAT and SOD.

The CAT, defined by the ability to cleave hydrogen peroxide into water and oxygen, was measured according to methodology proposed by Aebi (1984)[25]. The SOD activity, defined by the amount of enzyme that causes a reduction in the auto-oxidation of pyrogallol, was determined according to the methodology proposed by Dieterich et al. (2000)[26].

1.2.5.2. Histopathological processing

For histopathological and immunohistochemical analyses, the skin biopsy specimens were fixed in 10% buffered neutral formalin overnight, followed by dehydration through a graded series of ethanol concentrations. The samples were then cleared in xylene and embedded in paraffin baths before being molded into paraffin blocks, as described by Morais-Santos et al., (2018)[27]. Serial sections of 5 µm thickness were obtained using a Leica Multicut 2045 microtome (Reichert-Jung Products, Germany) and placed on silanized slides for immunohistochemical analysis and on standard glass slides for histological evaluation. The obtained slides were incubated in a 37ºC oven overnight to ensure complete drying and optimal adherence of the tissue sections to the glass. Histological parameters, including blood vessel density and epidermal thickness, were assessed using hematoxylin and eosin (HE) staining.[28] Mast cell quantification was performed using toluidine blue staining.[29] Differentiation of type I collagen fibers was achieved through Sirius Red staining [30].

1.2.5.3. Immunohistochemistry

Immunohistochemistry was performed to assess MG-induced tissue damage using markers of oxidative stress (8OHdG, 4HNE, catalase) and skin integrity (filaggrin), as described by Morais-Santos et al. (2018).[27]. Tissue sections (5 µm) were deparaffinized, rehydrated, washed in PBS, and subjected to endogenous peroxidase blocking to minimize nonspecific staining. Following antigen retrieval induced by heat treatment (20 minutes in a microwave) using sodium citrate buffer (0.1 M, pH 6.0), tissue sections were incubated with 5% BSA for one hour in a humid chamber to block nonspecific binding. After BSA removal, primary antibodies were applied: mouse anti-catalase [1:50, sc-271803], mouse anti-filaggrin [1:250, sc-66192], mouse anti-8OHdG [1:250, sc-393871] and goat anti-4HNE [1:50, AB5605]. The sections were then incubated overnight at 4°C in a humid chamber. Negative

controls were prepared by replacing the primary antibodies with PBS to confirm the specificity of the immunohistochemical reaction. After incubating, the sections were incubated with secondary antibodies - rabbit anti-goat (ab6721) for 4HNE detection and goat anti-mouse (12352203-Sigma) for catalase, filaggrin and 8OHdG - each conjugated to horseradish peroxidase (HRP), for 1 hour, followed by washing. Then, the slides were immersed in a developing solution containing 0.05% 3,3'-diaminobenzidine tetrahydrochloride (DAB) and 0.01% hydrogen peroxide in a Tris-HCl buffer (0.05 M, pH 7.4) to visualize the immunoreactivity. Finally, the sections were counterstained with Harris Hematoxylin.

1.2.5.4. Histological and Immunohistochemical sections analyses

The histological sections were captured at 40x magnification using a photomicroscope (EVOS™ M5000 Imaging System from Thermo Fisher Scientific) equipped with a digital camera (3® -QColor Olympus). A total of 10 images per slide were acquired for analysis, and tissue structures were manually quantified using a 300-point grid with the Image-Pro Plus 4.5 imaging software (Media Cybernetics, Silver Spring, USA). Epidermal thickness (in µm) was subsequently determined using the ImageJ version 1.53a software (National Institutes of Health, Rockville, MD, USA).

1.2.6. RNA Extraction and Quantitative Reverse Transcription PCR (RT-qPCR)

Skin samples were preserved in an RNA later solution (Invitrogen, Thermo Fisher Scientific) until processing. The samples were manually macerated in liquid nitrogen using a mortar and pestle to ensure tissue disruption for RNA extraction. Total RNA was then isolated using the PureLink™ RNA Mini Kit (Invitrogen, Thermo Fisher Scientific, Waltham, MA, USA), following the manufacturer's protocol. The macerated tissue was immediately homogenized in a lysis buffer containing 2-mercaptoethanol. The resulting lysate was clarified by centrifugation to remove cellular debris. RNA purification was performed by adding 70% ethanol to the supernatant and then transferring it to a spin column for selective RNA binding. The column was sequentially washed with the appropriate buffers, and total RNA was eluted in 20 µL of nuclease-free water. The quality and concentration of the extracted RNA were determined by spectrophotometry using the Multiskan SkyHigh system (Thermo Fisher Scientific, Waltham, MA, USA). Subsequently, 1 µg of total RNA from each

sample was reverse transcribed into cDNA using the High Capacity cDNA Reverse Transcription Kit (Thermo Fisher Scientific, Waltham, MA, USA). The mRNA expression levels of NFR-2 were quantified by real-time polymerase chain reaction (qPCR) using the PowerTrack™ SYBR™ Green Master Mix (Thermo Fisher Scientific, Waltham, MA, USA) on a QuantStudio™ 3 Real-Time PCR System (Thermo Fisher Scientific, Waltham, MA, USA), following the manufacturer's protocol. Gene expression was quantified based on the number of cycles required for each sample to reach its predetermined threshold value (Ct value). GAPDH was used as an internal reference gene for normalization. Data were analyzed using the relative standard curve method. The primers used in the real-time PCR assays had the following sequences: NRF-2-F: "TTC CCG GTC ACA TCG AGA G" NRF-2- R: " TCC TGT TGC ATA CCG TCT AAA TC" [31].

1.2.7. Statistical Analyses

Statistical analyses were performed using GraphPad Prism 8 software (GraphPad Software Inc., Boston, MA, USA). Data were expressed as mean and standard deviation (mean ± SD). The distribution of the data was assessed using the Kolmogorov-Smirnov test. For parametric data, comparisons were performed using one-way ANOVA, followed by the Tukey test. Non- parametric data were analyzed using the Kruskal-Wallis test. Statistical significance was defined as $p < 0.05$ for all analyses.

1.3. Results

1.3.1. Cell Viability

In the *in vitro* analyses, a decrease in cell viability in the MG1000 group was higher than the control group after 4h of exposure ($p<0.05$). In the MG 500 and MG 650 groups, there was no difference from the control group ($p>0.05$).

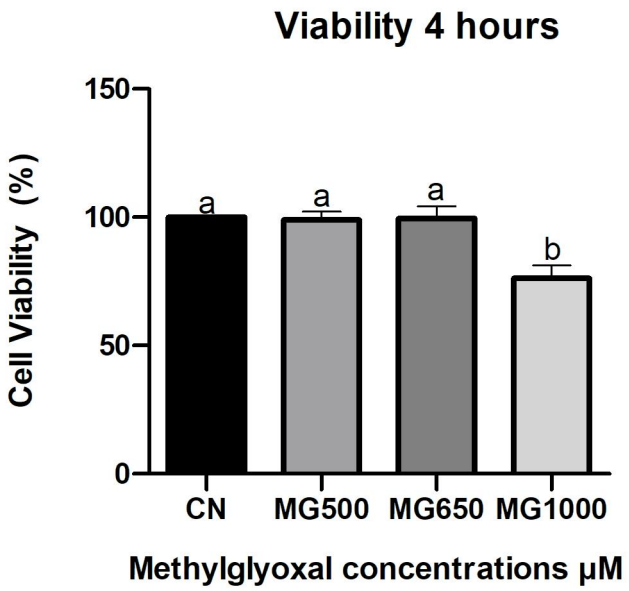

Figure 1. Cell viability at 4h after exposure to methylglyoxal at different concentrations. CN: control group, without methylglyoxal; MG500, MG650, and MG1000: exposure to methylglyoxal groups at concentrations of 500 µM, 650 µM, and 1000 µM, respectively.Different letters indicate statistically significant differences according to Tukey's post hoc test ($p < 0.05$).

1.3.2. Antioxidant Enzyme Activity *In Vitro*

There was an increase in the SOD enzyme activity in the MG650 group and a decrease in the MG500 group compared to the control group. The CAT activity enzymes increased the MG500 and MG1000 compared to the control group.

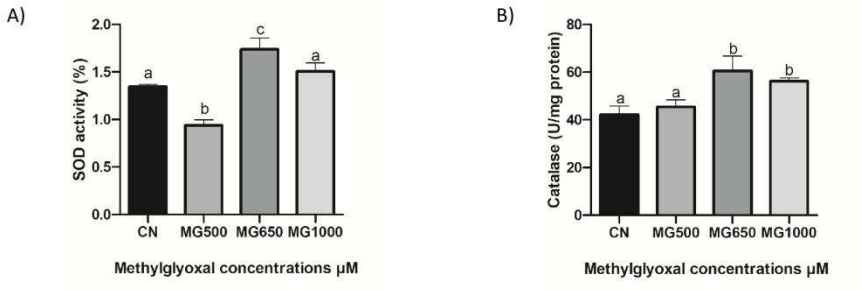

Figure 2. Antioxidant enzymes activity *in vitro*. (A) Superoxide dismutase (SOD) and (B) Catalase (CAT). CN: fibroblasts not exposed to methylglyoxal; MG500, MG650, and MG1000: fibroblasts exposed to methylglyoxal at concentrations of 500 µM, 650 µM, and 1000 µM, respectively. According to the Tukey test, groups with different letters exhibit statistically significant differences ($p<0.05$).

1.3.3. Antioxidant Enzymes Activity and Oxidative stress markers from cultured human skin fragments

There was an increase in the SOD enzyme activity in the MG650 group and MG500 group compared to the control group, with a more pronounced increase in the MG 650 group. The catalase activity enzymes increased in the MG650 group compared to the control group.

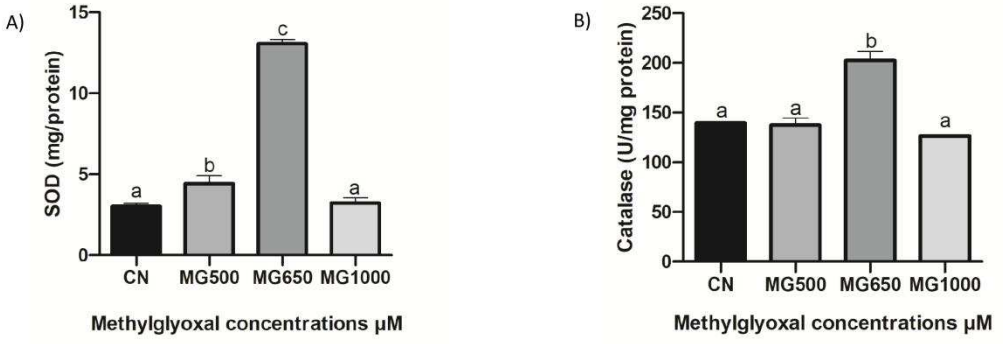

Figure 3. Effects of methylglyoxal administration at different concentrations on *ex vivo* skin samples. (A) Superoxide dismutase enzyme activity. (B) Catalase enzyme activity. CN: tissues without methylglyoxal exposure; MG500: tissues exposed to methylglyoxal at a concentration of 500 µM; MG650: tissues exposed to methylglyoxal at a concentration of 650 µM; MG1000: tissues exposed to methylglyoxal at a concentration of 1000 µM. According to the Tukey test, groups with different letters exhibit statistically significant differences ($p<0.05$).

1.3.4. Immunohistochemistry

In immunohistochemistry, the filaggrin immunomarker decreased after MG exposure at all concentrations, with the worst results presented after MG500, MG1000 and MG 650 exposure, respectively (Figure 4). There was an increase in catalase activity after exposure to MG650 compared to all groups (Figure 5). Immunostaining of the 8OHdG was higher at the MG650 and MG1000 concentrations, with a more pronounced increase in the MG1000 group (Figure 6). 4-HNE immunostaining revealed an increase compared to the control at MG 650 and MG 1000 concentrations. No significant difference was observed at MG 500 relative to the negative control. (Figure 7).

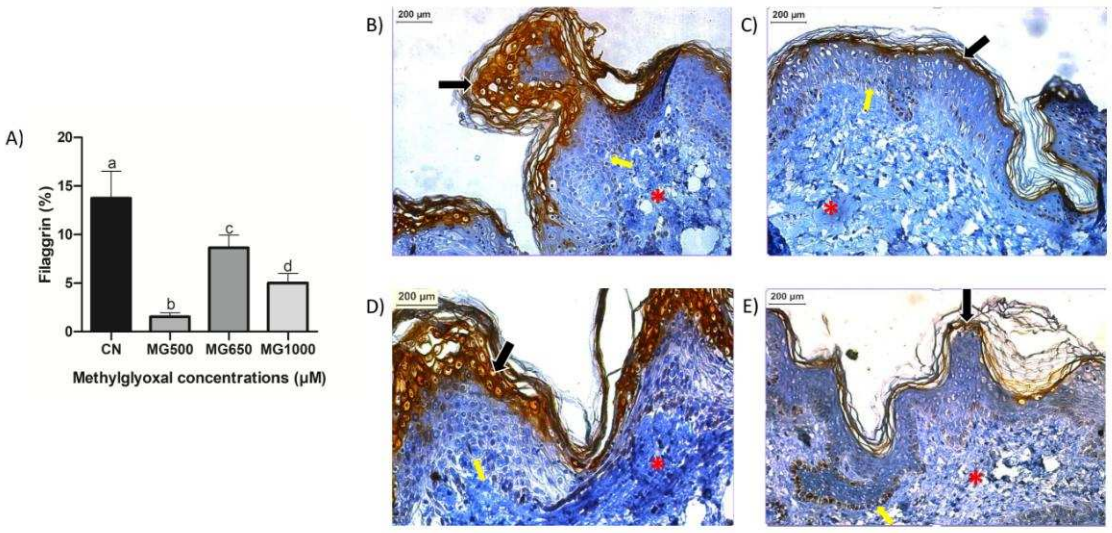

Figure 4. Quantification of immunostaining for filaggrin (A) in *ex vivo* skin fragments exposed to different concentrations of methylglyoxal. CN: skin fragments not exposed to methylglyoxal (culture medium only); MG500: skin fragments exposed to methylglyoxal at a concentration of 500 µM; MG650: skin fragments exposed to methylglyoxal at a concentration of 650 µM; MG1000: skin fragments exposed to methylglyoxal at a concentration of 1000 µM. According to the Tukey test, groups with different letters exhibit statistically significant differences ($p<0.05$). B-E Photomicrograph of skin with immunohistochemical staining for filaggrin. Control group = Skin fragments not exposed to methylglyoxal (B), skin fragments exposed to methylglyoxal at concentrations of 500 µM (C), 650 µM (D), and 1000 µM (E). Black arrows: filaggrin immunostaining; yellow arrows: epidermis; red asterisks: dermis. Scale bar = 200 µm.

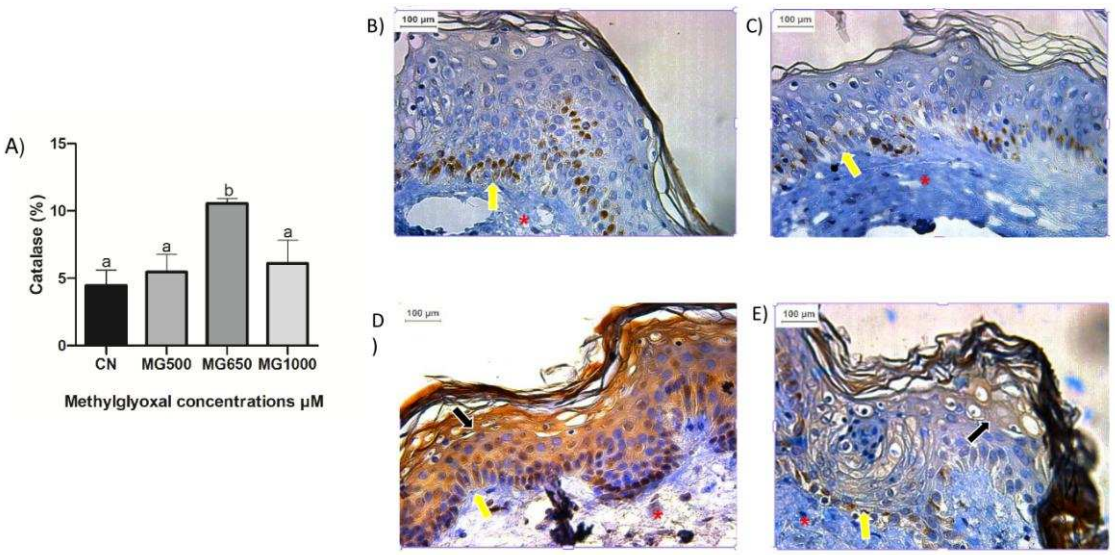

Figure 5. Quantification of immunostaining for catalase enzyme (A) in *ex vivo* skin fragments exposed to different concentrations of methylglyoxal. CN: skin fragments not exposed to methylglyoxal (culture medium only); MG500: skin fragments exposed to methylglyoxal at a concentration of 500 µM; MG650: skin fragments exposed to methylglyoxal at a concentration of 650 µM; MG1000: skin fragments exposed to methylglyoxal at a concentration of 1000 µM. According to the Tukey test, groups with different letters exhibit statistically significant differences ($p<0.05$). B-E Photomicrograph of skin with immunohistochemical staining for catalase. Control group = Skin fragments not exposed to methylglyoxal (A); skin fragments exposed to methylglyoxal at concentrations of 500 µM (B); skin fragments exposed to methylglyoxal at concentrations of 650 µM (C); skin fragments exposed to methylglyoxal at concentrations of 1000 µM (D). Black arrows: immunostaining for catalase in epidermis; yellow arrows: epidermis; red asterisks: dermis. Scale bar = 100 µm.

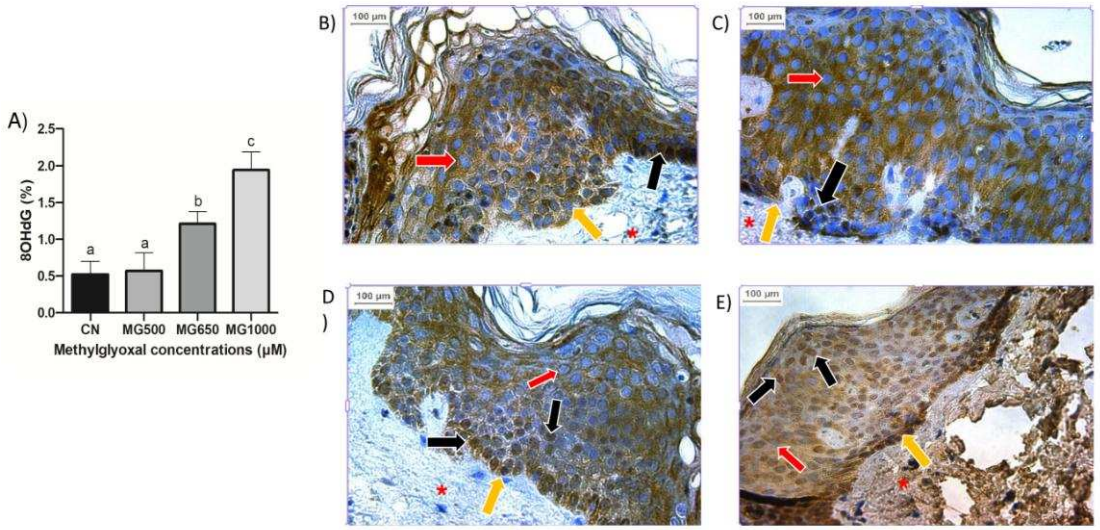

Figure 6. Quantification of immunostaining for 8 OHdG (A) in *ex vivo* skin fragments exposed to different concentrations of methylglyoxal. CN: skin fragments not exposed to methylglyoxal (culture medium only); MG500: skin fragments exposed to methylglyoxal at a concentration of 500 µM; MG650: skin fragments exposed to methylglyoxal at a concentration of 650 µM; MG1000: skin fragments exposed to methylglyoxal at a concentration of 1000 µM. According to the Tukey test, groups with different letters exhibit statistically significant differences ($p<0.05$). B-E Photomicrograph of skin with immunohistochemical staining for 8 OHdG. Control group = Skin fragments not exposed to methylglyoxal (A); skin fragments exposed to methylglyoxal at concentrations of 500 µM (B); skin fragments exposed to methylglyoxal at concentrations of 650 µM (C); skin fragments exposed to methylglyoxal at concentrations of 1000 µM (D). Black arrowheads: immunostained cell nuclei; red arrowheads: normal cell nuclei;yellow arrows: epidermis; red asterisks: dermis. Scale bar = 100

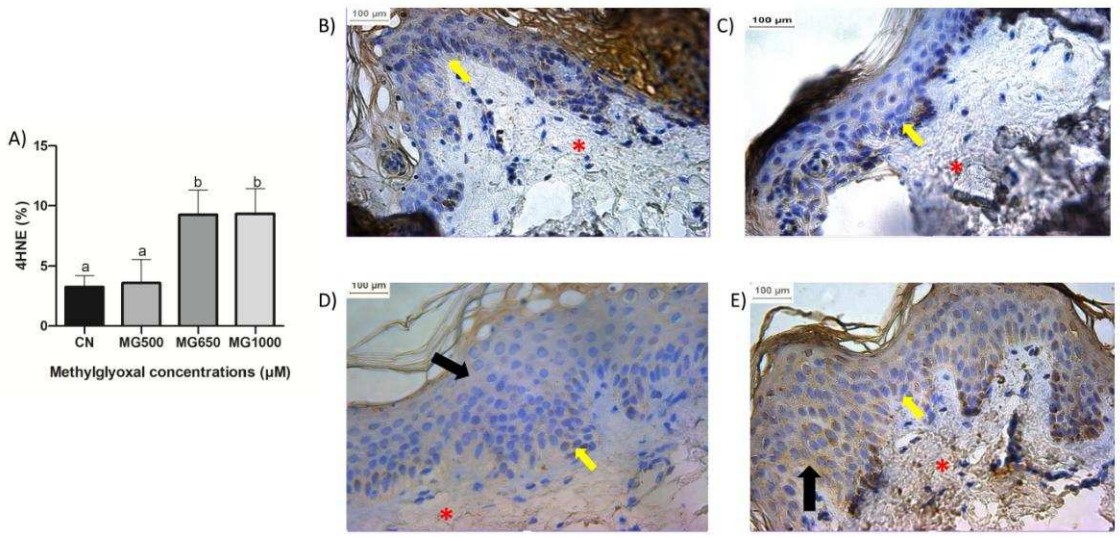

µm. **F**

igure 7. Quantification of immunostaining for 4HNE (A) in *ex vivo* skin fragments exposed to different concentrations of methylglyoxal. CN: skin fragments not exposed to methylglyoxal (culture medium only); MG500: skin fragments exposed to methylglyoxal at a concentration of 500 µM; MG650: skin fragments exposed to methylglyoxal at a concentration of 650 µM; MG1000: skin fragments exposed to methylglyoxal at a concentration of 1000 µM. According to the Tukey test, groups with different letters exhibit statistically significant differences ($p<0.05$). B-E Photomicrograph of skin with immunohistochemical staining for 4HNE. Control group = Skin fragments not exposed to methylglyoxal (B); skin fragments exposed to methylglyoxal at concentrations 500 µM (C); skin fragments exposed to methylglyoxal at concentrations 650 µM (D); skin fragments exposed to methylglyoxal at concentrations 1000 µM (E). Black arrows: immunostaining for 4HNE in epidermis.yellow arrows: epidermis; red asterisks: dermis. Scale bar = 100 µm.

1.3.5. Histological Analyses

In the histochemical analyses, we observed a decrease in type I collagen levels at MG 500 and MG 650 concentrations compared to the control group (Figure 8).

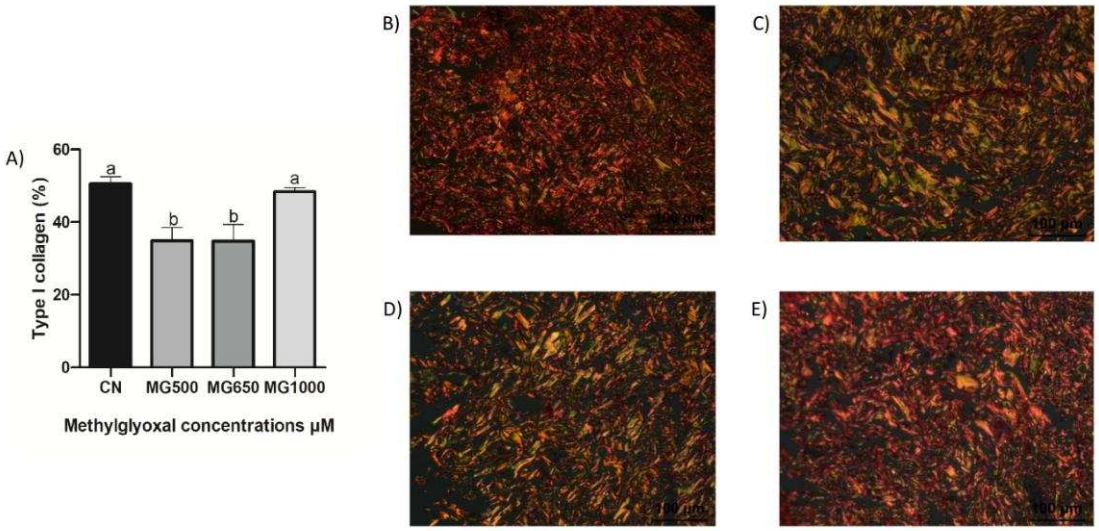

Figure 8. Effects of different concentrations of methylglyoxal on the structural protein of the dermis in skin fragments. (A) Percentage of type I collagen. CN: skin fragments without exposure to methylglyoxal (culture medium only); MG500: fragments exposed to methylglyoxal at a concentration of 500 µM; MG650: fragments exposed to methylglyoxal at a concentration of 650 µM; MG1000: fragments exposed to methylglyoxal at a concentration of 1000 µM. According to the Tukey test, groups with different letters exhibit statistically significant differences ($p<0.05$). (B,C,D and E) Photomicrograph of epithelial tissue stained with Sirius Red type I collagen. Control group = Skin fragments not exposed to methylglyoxal (B); skin fragments exposed to methylglyoxal at concentrations 500 µM (C); skin fragments exposed to methylglyoxal at concentrations 650 µM (D); skin fragments exposed to methylglyoxal at concentrations 1000 µM (E). Orange or red staining indicates type I collagen. Scale bar = 100 µm

A higher density of mast cells was observed in the dermis of skin fragments at the 500 µM concentration of methylglyoxal, while the concentrations of 650 and 1000 µM showed no significant differences compared to the control group. However, MG1000 group exhibited a statistically significant difference from the MG500 group, displaying a lower mast cell density (Figure 9).

Figure 9. Effects of different concentrations of methylglyoxal on the number of mast cells in skin fragments. CN: skin fragments without methylglyoxal (only culture medium); MG500: skin fragments containing methylglyoxal at a concentration of 500 μM; MG650: skin fragments containing methylglyoxal at a concentration of 650 μM; MG1000: skin fragments containing methylglyoxal at a concentration of 1000 μM. The presence of different letters (a,b) in the columns indicates statistically significant differences ($p<0.05$) between groups. According to the Tukey test, groups with different letters exhibit statistically significant differences ($p<0.05$), highlighting the practical relevance of our findings.

Regarding the proportion of blood vessels, a higher amount of these components was detected in the skin fragments exposed to the 500 and 650 μM of methylglyoxal exposure compared to the control group (Figure 10 A). In the investigation of the interference of methylglyoxal on epidermal thickness, no significant changes were observed at any concentration of the stressor agent (Figure 10 B).

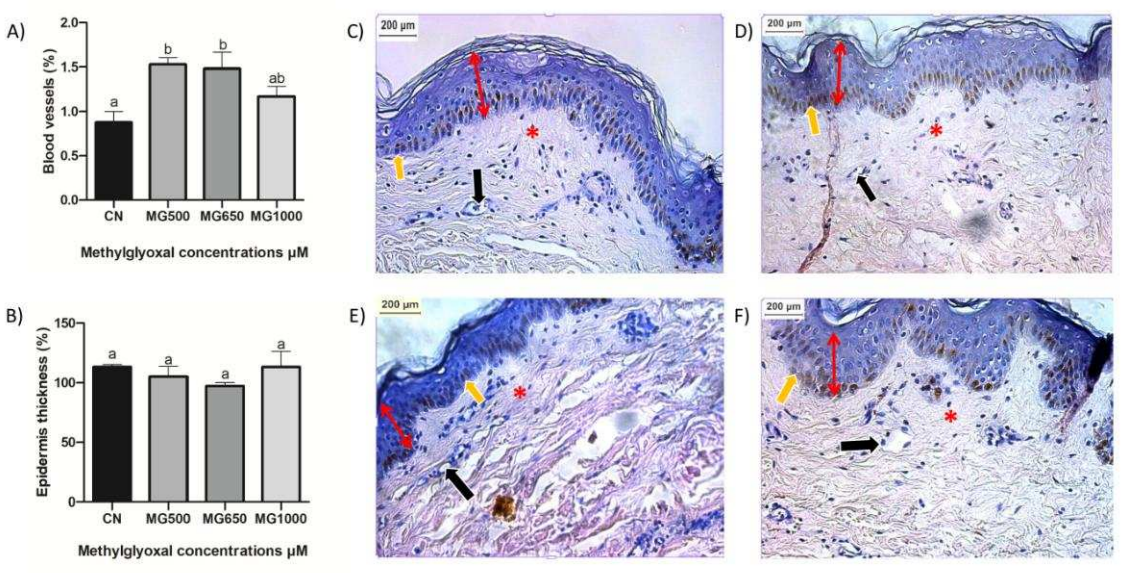

Figure 10. Percentage of blood vessels (A) and epidermal thickness (B) in histological sections. CN: skin fragments without methylglyoxal (culture medium only); MG500: skin fragments containing methylglyoxal at a concentration of 500 µM; MG650: skin fragments containing methylglyoxal at a concentration of 650 µM; MG1000: skin fragments containing methylglyoxal at a concentration of 1000 µM. According to the Tukey test, groups with different letters exhibit statistically significant differences ($p<0.05$). C-F photomicrograph of skin stained with hematoxylin and eosin. Skin fragments are not exposed to methylglyoxal (C); skin fragment exposed to methylglyoxal at concentrations of 500 µM (D); skin fragment exposed to methylglyoxal at concentrations of 650 µM (E); skin fragment exposed to methylglyoxal at concentrations of 1000 µM (F). Yellow arrows: epidermis; red asterisks: dermis; black arrowheads: blood vessels; double red arrows: epidermal thickness; Scale bar = 200 µm.

1.3.6. NRF2 Expression

Through molecular analysis, we observed that the use of methylglyoxal at the three chosen concentrations resulted in an approximately 1.5-fold increase in the expression of transcription factor NRF2, responsible for regulating the cellular antioxidant response, at concentrations of 650 and 1000 µM, with a more pronounced effect at the 650 µM concentration compared to the control group (Figure 11).

Figure 11. Graph bars indicate NRF2 gene expression. CN: control sample, without methylglyoxal; MG500: sample containing methylglyoxal at a concentration of 500 μM; MG650: sample containing methylglyoxal at a concentration of 650 μM; MG1000: sample containing methylglyoxal at a concentration of 1000 μM. According to the Tukey`s test, groups with different letters (a,b) exhibit statistically significant differences ($p<0.05$).

1.4. Discussion

MG is a highly reactive dicarbonyl compound physiologically produced by cells as a byproduct of glucose metabolism, particularly during glycolysis.[32] Its excessive accumulation has been associated with several pathologies, especially related to pathological processes, including oxidative stress and inflammation responsible for cellular apoptosis, biomolecular damage, and gene expression modulation [33]. Additionally, MG plays a key role in forming AGEs, which contribute to cellular aging and the development of chronic diseases[34]. However, despite the growing recognition of MG's systemic impact, there is still no consensus in the literature regarding its physiological and pathological concentrations in the skin nor its specific effects on cell viability and the functional integrity of cutaneous tissue. Therefore, our study aimed to elucidate the interaction of different concentrations of MGO and its consequences for the skin.

In the present study, we assessed the cytotoxic effects of varying MG concentrations in dermal fibroblasts following exposure durations of 4 hours. Our findings indicate that exposure to 1000 μM MG significantly reduced cell viability after 4 hours, suggesting that this concentration elicits an acute cellular response and permanent damage to the cells. These

results are consistent with the findings of Prestes et al. (2022)[35], who reported that mitochondria of cells exposed to elevated MG concentrations (0.1-10 mM) for a short duration exhibited decreased viability and disruption of mitochondrial membrane potential. In contrast, no significant changes in viability were observed at 500 μM and 650 μM at this time point.

After analyzing the reduction in cell viability in fibroblasts, the next step was to investigate the potential of different MG concentrations to induce oxidative stress, as previously reported by Wang et al., (2022)[36]. SOD and CAT activity were measured *in vitro* and *ex vivo.* The observed reduction in cell viability, especially with 1000 μM MG exposure, may be linked to the alterations induced by oxidative stress. Notably, *in vitro*, the increase in SOD activity at 650 μM and the increase in catalase activity at both 650 μM and 1000 μM suggest that the cells are activating their antioxidant defenses in response to oxidative damage. The immunohistochemical analyses that were done in our study proved that after 650 μM MG exposure, the antioxidant enzyme system was activated, without promoting enzymatic exhaustion. Conversely, the decrease in SOD activity at 500 μM suggests a less effective antioxidant response. These findings highlight how cellular stress induced by MG exposure can impair metabolic pathways and cellular function. In the *ex vivo* skin analysis, a similar oxidative stress response was observed. Under normal conditions, when there is an increase in markers of oxidative damage, antioxidant systems are activated to combat free radicals, reducing signs of oxidative stress in tissues. However, when the impact of an aggressive agent is too strong, the antioxidant systems may not be sufficient to neutralize the excessive production of reactive oxygen species (ROS), which can lead to morphological and functional changes in the tissues.[37]

Given the oxidative stress and metabolic changes induced by MG exposure, we evaluated the expression of key markers involved in skin integrity and cellular response in *ex vivo* tissue samples. The markers assessed were filaggrin, a fundamental structural protein rich in histidine, abundantly present in keratinocytes during their final maturation stages. It is derived from profilaggrin, which, during the terminal differentiation of keratinocytes, is phosphorylated to produce filaggrin.[38] This protein is crucial for developing and maintaining the skin barrier and forming corneocytes. Its cellular levels are regulated by genetic factors, inflammatory processes, and stress agents.[39] A deficiency in filaggrin results in various biochemical and physiological alterations in the skin barrier, impairing its protective function against environmental factors and water loss. For instance, this deficiency can lead to the release of pro-inflammatory factors by keratinocytes, triggering an inflammatory response.[40]

Despite its importance in skin homeostasis, filaggrin accumulation can be harmful, disrupting intermediate filaments, breaking cell junctions, and leading to programmed cell death.[41] Filaggrin expression increases during normal keratinocyte differentiation until it reaches a local concentration limit. Once this limit is exceeded, unsequestered profilaggrin molecules can escape into the cytosol, forming bonds and becoming active. Because high levels of this protein need to be regulated, an active mechanism removes excess unsequestered profilaggrins during cellular differentiation to prevent potential damage.[42] In our results, the negative control, representing normal skin conditions, showed a high presence of filaggrin. However, this rate reduced drastically to a concentration of 500 μM of methylglyoxal. This result suggests that the cells activated the active mechanism for removing excess unsequestered profilaggrin during methylglyoxal-induced stress, decreasing protein levels. At higher concentrations of the stress agent, it is possible that the cellular protective system was overwhelmed and unable to adequately remove unsequestered molecules. These molecules likely became reactivated, forming filaggrin again, but without reaching the normal levels observed in the negative control.

In the immunohistochemical assays, we also analyzed the presence of nuclear damage through labeling with the anti-8-hydroxyguanosine (8-OHdG) antibody, an RNA nucleoside resulting from the oxidation of guanosine.[43] This oxidation generates the compound 8-hydroxy-2'-deoxyguanosine, which serves as a marker for oxidative damage in DNA molecules.[44] In our results, we observed that the levels of this marker were significantly upregulated at concentrations of 650 and 1000 μM, compared to the control. We believe that the oxidative damage to DNA molecules at higher concentrations of MG is related to the known ability of this compound to interact with arginine and lysine molecules, causing post-translational modifications that affect the stability, structure, and function of proteins crucial for maintaining genomic integrity, such as histones.[45] The 500 μM concentration did not show significant differences from the control, which we believe is due to the efficiency of the glyoxalase system in metabolizing the compound, under conditions closer to physiological normality, acting as a dose-dependent defense mechanism.[46]

Furthermore, we analyzed the presence of 4-hydroxy-2-nonenal (4HNE), an important and indicative of lipid peroxidation (LPO). Fatty acids undergo autooxidation under oxidative stress conditions, forming highly reactive carbonyl species (RCS) that can interact with and modify biological macromolecules, altering their structure and function.[47] In our studies, we analyzed the presence of the 4HNE compound through immunohistochemical analysis, and we observed a significant increase after 650 and 1000 MG exposure These findings support

our other previously discussed results regarding the higher oxidative stress at these two concentrations and show us that the lipid peroxidation is higher in these concentrations, probably due to the increase in free radicals and ROS production. On the other hand, the 500 µM concentration did not show a significant difference from the control. We believe that, at this concentration, the antioxidant mechanisms, including the GSH enzyme, which is capable of neutralizing RCS, managed to detoxify most of the reactive molecules in the tissue. [48]

Type I collagen fibers are essential for maintaining the normal architecture of the extracellular matrix in connective tissue, providing resistance to mechanical forces.[49] Type I collagen is the most abundant protein in human skin, organizing with fibrillar collagens, such as types III and V, to form larger collagen fibers. These fibers create a network that sustains mechanical tension supplied by fibroblasts, which produce them, thus maintaining skin health. Oxidative damage results in irreversible functional impairment of fibroblasts and is a major contributor to skin aging. Under stress conditions, excessive collagen fragmentation leads to reduced collagen production by skin fibroblasts.[50] Moreover, disturbances in the fibroblast microenvironment reduce their mechanical tension, potentially causing fibroblast collapse, thereby reducing skin collagen levels. This process is accompanied by an increase in collagenase levels, which degrade the accumulated collagen.[51] As discussed earlier, MG damages the skin tissue by inducing an excessive production of reactive oxygen species (ROS), leading to oxidative stress.

As previously mentioned, MG is a precursor in the formation of AGEs. When collagen interacts with these AGEs, chemical modifications occur, leading to the formation of irreversible cross-links between collagen fibers. This process compromises the structural organization of the extracellular matrix, resulting in fiber deformation and the loss of biomechanical properties.[52] These effects justify the reduction in type I collagen levels observed at MG concentrations of 500 µM and 650 µM, as the increased cross-linking impairs collagen synthesis and homeostasis. Moreover, exposure to high concentrations of MG can interfere with collagen degradation, as the irreversible modification of proteins may impair the activity of enzymes responsible for this process, such as matrix metalloproteinases (MMPs) and hyaluronidase. This mechanism may explain why, at a concentration of 1000 µM of MG, type I collagen levels remained similar to those of the control group, suggesting a compensatory effect within the extracellular matrix.

Another histological criterion we analyzed was the presence and quantification of mast cells, understanding that these cells play an important role in both physiological and pathological processes and mediate allergic reactions. They originate from mononuclear

precursors in the bone marrow, migrate, and undergo differentiation in situ, influenced by local tissue cytokines.[53] In the skin, mast cells are found in the dermis, distributed around blood vessels, and can migrate to the epidermis in response to certain pathologies.[54] Another significant role of these cells is in inflammation, activated by non-allergic triggers, releasing pro-inflammatory mediators.[55] The release of these mediators recruits other inflammatory cells; however, this mechanism can be detrimental to tissue due to an exaggerated inflammatory response.[56] In our study, we observed that the concentration of 500 μM methylglyoxal increased the levels of mast cells found in the skin. This increase can be attributed to the inflammatory process induced by MG. However, at higher concentrations of the stressor, the levels of mast cells remained similar to those in the control group, indicating that further studies are needed to understand the mechanisms activated by the cells at these concentrations.

Our findings on blood vessels formation indicate a significant increase in angiogenesis at MG concentrations of 500 μM and 650 μM compared to the control group. Angiogenesis is an important process for maintaining microvasculature and, consequently, for tissue health. This process is directly regulated by growth factors, and their reduced availability can impair angiogenesis.[57] One essential growth factor for angiogenesis is transforming growth factor-beta (TGF-β) and its co-receptor, the molecule endoglin, which promotes endothelial proliferation and migration, supporting vessel survival. Endoglin is known to be present at high levels in inflamed tissues, indicating an endothelial repair strategy and the formation of new blood vessels as an attempt to support tissue survival.[58] Based on our findings, we suggest an attempt to mitigate inflammation and ensure tissue survival in response to the stress caused by methylglyoxal, enhancing white blood cell infiltration at the site of inflammation.[59] Our results also indicate no histological alterations in epidermal thickness. The epidermis, as the outermost layer of the skin, playing a crucial role as a protective barrier against harmful environmental agents and regulating water and electrolyte loss, preventing dehydration.[60] Its morphology is directly related to its function, where increased rigidity reduces its ability to deform.[61] A reduction in epidermal thickness and structural changes contribute to skin fragility, increasing the risk of injuries such as skin lacerations.[62] Therefore, our results suggest that methylglyoxal did not induce significant structural damage to the epidermis.

The effects of stress-inducing agents, such as methylglyoxal (MG), activate redox-sensitive transcription factors like Nuclear Factor Erythroid 2-Related Factor 2 (NRF2) and cellular survival pathways.[63] NRF2 plays a crucial role in upregulating cellular defense

mechanisms against oxidative damage by upregulating the expression of antioxidant and detoxification enzymes. Under stress conditions, NRF2 translocates to the nucleus and binds to antioxidant response elements (AREs) within the promoter regions of target genes, thereby mitigating oxidative stress, inhibiting apoptosis, and promoting cellular survival.[64] Consistent with these findings, our data suggest that NRF2 was overexpressed in response to MG-induced stress, particularly at a concentration of 650 µM, which correlated with increased levels of antioxidant enzymes. However, despite the upregulation of NRF2 at 1000 µM MG, antioxidant enzymes levels remained, in most assays, comparable to those observed in the control group. This suggests a possible saturation or impairment of the antioxidant response at higher MG concentrations. When a cell is exposed to stress beyond its threshold, it activates programmed cell death pathways.[65] We observed this process in some tests conducted with the 1000 µM concentration of methylglyoxal, where cell survival rates were significantly lower than at the other concentrations. The overexpression of NRF2 at the 650 µM concentration allowed us to observe the expression of anti-apoptotic genes involved in ROS elimination, in an attempt to delay and/or prevent cell death.

In the figure below, we illustrate the action process of methylglyoxal on epithelial tissue cells and highlight the main results found.

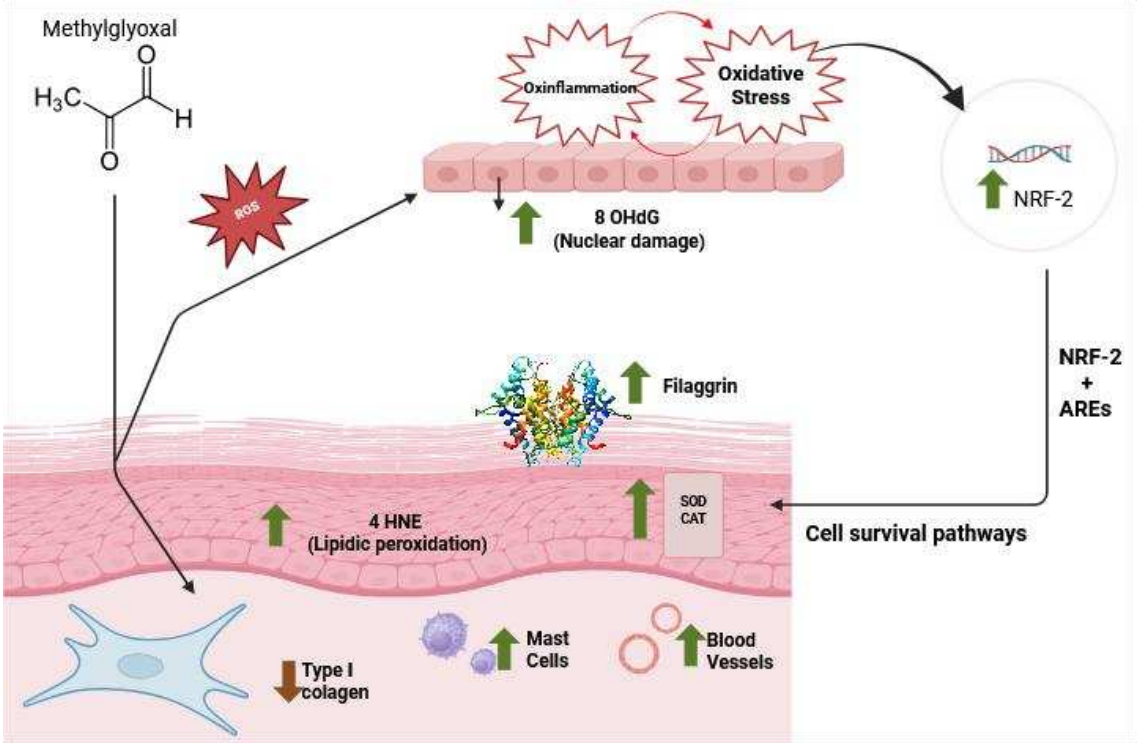

Figure 12. Final summary of main results found

1.5. Conclusion

Our findings help to elucidate the consequences caused by methylglyoxal in skin tissue. As observed, the concentration of 650 μM of methylglyoxal inducing stress in both ex vivo and cell culture experiments. At this concentration, tissue stress was evident while maintaining cell viability. This effect could be associated with an increase in NRF2 expression, leading to the upregulation of antioxidant enzymes, as well as enhanced filaggrin expression and blood vessel responses to stress. Although the 500 μM concentration induced some stress while preserving cell viability, it did not produce significant differences compared to the control in several assays. In contrast, the 1000 μM concentration resulted in substantial tissue damage, preventing further experimentation.

Funding

This work was supported by the Brazilian agencies: Fundação de Amparo à Pesquisa do Estado de Minas Gerais (FAPEMIG, processAPQ-03519-22 and APQ-04164-22), Coordenação de Aperfeiçoamento de Pessoal de Nível SuperiorBrasil (CAPES, Finance Code 001), and Conselho Nacional de Desenvolvimento Científico e Tecnológico (CNPq, processes 310413/2023-0, 306733/2023-4, and 403194/2023-7).

Acknowledgments:

This work was supported by the Laboratory of Experimental Pathology at the Federal University of Viçosa.

Data availability statement

The datasets used or analyzed during the current study are available from the corresponding author on reasonable request.

Author contributions: CRediT

Caroline Massardi: Conceptualization, Data Curation, Formal analysis, Investigation, Methodology, Visualization, Writhing - original draft. **Eduarda Costa**: Data Curation, Investigation, Methodology, Writhing - original draft. **Monica Morais:** Methodology, Project administration, Writing - review and editing. **Manoela Maciel:** Supervision, Validation, Writing - review and editing. **Rosineia de Paula:** Methodology, Software, Validation. **Carlos**

Eduardo: Methodology, Resources. **Giuseppe Valacchi**: Metodology, Writing - review and editing. **Reggiani Vilela Gonçalves**: Funding acquisition, Project administration, Resources, Supervision, Visualization, Writing - review and editing.

1.6. References

1. Woodby, Brittany et al. Skin health from the inside out. **Annual review of food science and technology**, v. 11, n. 1, p. 235-254, 2020.

2. Ivarsson, John et al. Comparison of pollutant effects on cutaneous inflammasomes activation. **International Journal of Molecular Sciences**, v. 24, n. 23, p. 16674, 2023.

3. Baek, Jinok; Lee, Min-Geol. Oxidative stress and antioxidant strategies in dermatology. **RedoxReport,** v. 21, n. 4, p. 164-169, 2016.

4. Farris, Patricia K.; Valacchi, Giuseppe. Ultraviolet light protection: is it really enough?. **Antioxidants**, v. 11, n. 8, p. 1484, 2022.

5. Valacchi, G. et al. Ox-Inflammation: from subclinical condition to pathological biomarker. **Front. Physiol**. 9: e858. 2018.

6. Sruthi, C. R.; Raghu, K. G. Advanced glycation end products and their adverse effects: the role of autophagy. **Journal of Biochemical and Molecular Toxicology**, v. 35, n. 4, p. e22710, 2021.

7. Singh, R. B. A. M. et al. Advanced glycation end-products: a review. Diabetologia, v. 44, p. 129-146, 2001.

8. Desai, Kaushik M. et al. Oxidative stress and aging: is methylglyoxal the hidden enemy? **Canadian journal of physiology and pharmacology**, v. 88, n. 3, p. 273-284, 2010.

9. Thornalley, Paul J. Pharmacology of methylglyoxal: formation, modification of proteins and nucleic acids, and enzymatic detoxification-a role in pathogenesis and antiproliferative chemotherapy. **General Pharmacology: The Vascular System**, v. 27, n. 4, p. 565-573, 1996.

10. Yang, Chun-tao et al. A novel controllable hydrogen sulfide-releasing molecule protects human skin keratinocytes against methylglyoxal-induced injury and dysfunction. **Cellular Physiology and Biochemistry**, v. 34, n. 4, p. 1304-1317, 2014.

11. Polykretis, Panagis et al. Methylglyoxal interaction with superoxide dismutase 1. **Redox biology**, v. 30, p. 101421, 2020.

12. Lo, T. W. et al. Binding and modification of proteins by methylglyoxal under

physiological conditions. A kinetic and mechanistic study with N alpha-acetylarginine, N alpha- acetylcysteine, and N alpha-acetyllysine, and bovine serum albumin. **Journal of Biological Chemistry**, v. 269, n. 51, p. 32299-32305, 1994.

13. Rabbani, Naila; Thornalley, Paul J. Dicarbonyls linked to damage in the powerhouse: glycation of mitochondrial proteins and oxidative stress. 2008.

14. Yumnam, Silvia; Subedi, Lalita; Kim, Sun Yeou. Glyoxalase system in the progression of skin aging and skin malignancies. **International Journal of Molecular Sciences**, v. 22, n. 1, p. 310, 2020.

15. Shutova, Maria S.; Boehncke, Wolf-Henning. Mechanotransduction in skin inflammation. **Cells**, v. 11, n. 13, p. 2026, 2022.

16. Lopes, Fernanda Barbosa et al. OxInflammatory responses in the wound healing process: a systematic review. **Antioxidants**, v. 13, n. 7, p. 823, 2024.

17. Silveira, Leonardo L. et al. OxInflammation Affects Transdifferentiation to Myofibroblasts, Prolonging Wound Healing in Diabetes: A Systematic Review. **International Journal of Molecular Sciences**, v. 25, n. 16, p. 8992, 2024.

18. Costa, E.P., Santos, M.M., Paula, R.A., Silva, D.A., Lopes, R.P., Teixeira, R.R., Gonçalves, R.V., 2025. Antioxidant and Anti-inflammatory Activity of Eugenol, Bis-eugenol, and Clove Essential Oil: An In Vitro Study. **ACS Omega,** Article ASAP**.** https://doi.org/10.1021/acsomega.5c04146

19. Gonçalves, Reggiani Vilela; Costa, Andrea MA; Grzeskowiak, Lukasz. Oxidative stress and tissue repair: mechanism, biomarkers, and therapeutics. **Oxidative Medicine and Cellular Longevity**, v. 2021, 2021

20. Benedusi, Mascia et al. Oxidative State in Cutaneous Melanoma Progression: A Question of Balance. **Antioxidants**, v. 13, n. 9, p. 1058, 2024.

21. Neil, MS Jessica E. et al. A new ex vivo skin model for mechanistic understanding of putative anti-inflammatory topical therapeutics. **International Journal of Pharmaceutics**, v. 617, p. 121610, 2022.

22. Ferrara, Francesca et al. Redox regulation of cutaneous inflammasome by ozone exposure. **Free Radical Biology and Medicine**, v. 152, p. 561-570, 2020.

23. VALACCHI, Giuseppe et al. Particulate matter induces tissue oxinflammation: from mechanism to damage. **Antioxidants & Redox Signaling**, v. 33, n. 4, p. 308-326, 2020.

24. MU, Lixian et al. A potential wound-healing-promoting peptide from salamander skin. **The FASEB journal**, v. 28, n. 9, p. 3919, 2014.

25. AEBI, Hugo. Catalase in vitro. In: **Methods in enzymology**. Academic press, 1984. p. 121-126.

26. Dieterich S, Bieligk U, Beulich K, Hasenfuss G, Prestle J. Gene Expression of Antioxidative Enzymes in the Human Heart. **Circulation.** 2000;101: 33–39. doi:10.1161/01.CIR.101.1.33.

27. Morais-santos, Monica et al. Basal cells show increased expression of aromatase and estrogen receptor α in prostate epithelial lesions of male aging rats. **Endocrinology**, v. 159, n. 2, p. 723-732, 2018.

28. Gonçalves R V., Novaes RD, Matta SLP, Benevides GP, Faria FR, Pinto MVM. Comparative Study of the Effects of Gallium-Aluminum-Arsenide Laser Photobiomodulation and Healing Oil on Skin Wounds in Wistar Rats: A Histomorphometric Study. **Photomed Laser Surg**. 2010;28: 597–602. doi:10.1089/pho.2009.2669.

29. Churukian CJ, Schenk EA. A Toluidine Blue Method for Demonstrating Mast Cells. **J Histotechnol.** 1981;4: 85–86. doi:10.1179/his.1981.4.2.85.

30. Cupertino MC, Costa KLC, Santos DCM, Novaes RD, Condessa SS, Neves AC, et al. Long-lasting morphofunctional remodelling of liver parenchyma and stroma after a single exposure to low and moderate doses of cadmium in rats. **Int J Exp Pathol**. 2013;94: 343–351. doi:10.1111/iep.12046.

31. Golpour, Pegah et al. Improvement of NRF2 gene expression and antioxidant status in patients with type 2 diabetes mellitus after supplementation with omega-3 polyunsaturated fatty acids: A double-blind randomised placebo-controlled clinical trial. **Diabetes Research and Clinical Practice**, v. 162, p. 108120, 2020.

32. Yousif A. Shamsaldeen, Louise S. Mackenzie, Lisa A. Lione, Christopher D. Benham, Methylglyoxal, A Metabolite Increased in Diabetes is Associated with Insulin Resistance, Vascular Dysfunction and Neuropathies, Current Drug Metabolism; Volume 17, Issue 4, Year 2016. DOI: 10.2174/1389200217666151222155216.

33. Chan, C.-M., Huang, D.-Y., Huang, Y.-P., Hsu, S.-H., Kang, L.-Y., Shen, C.-M. and Lin, W. W. (2016), Methylglyoxal induces cell death through endoplasmic reticulum stress-associated ROS production and mitochondrial dysfunction. **J. Cell. Mol. Med**., 20: 1749- 1760. https://doi.org/10.1111/jcmm.12893.

34. Sheng J, Liu C, Petrovas S, Wan Y, Chen HD, Seeram NP, Ma H. Phenolic-enriched maple syrup extract protects human keratinocytes against hydrogen peroxide and methylglyoxal induced cytotoxicity. **Dermatol Ther.** 2020 May;33(3):e13426. doi: 10.1111/dth.13426. Epub 2020 May 3. PMID: 32301192; PMCID: PMC7880121.

35. Prestes AS, Dos Santos MM, Kamdem JP, Mancini G, Schüler da Silva LC, de Bem AF, Barbosa NV. Methylglyoxal disrupts the functionality of rat liver mitochondria. **Chem Biol Interact**. 2022 Jan 5;351:109677. doi: 10.1016/j.cbi.2021.109677. Epub 2021 Oct 8. PMID:34634269.

36. Wang, Gang et al. Metformin prevents methylglyoxal-induced apoptosis by suppressing oxidative stress in vitro and in vivo. **Cell Death & Disease**, v. 13, n. 1, p. 29, 2022.

37. Rosa DF, Sarandy MM, Novaes RD, Freitas MB, do Carmo Gouveia Pelúzio M, Gonçalves RV. High-Fat Diet and Alcohol Intake Promotes Inflammation and Impairs Skin Wound Healing in Wistar Rats. **Mediators Inflamm**. 2018 Jul 24;2018:4658583. doi: 10.1155/2018/4658583. PMID: 30140168; PMCID: PMC6081583.

38. Hoober, J. Kenneth; Eggink, Laura L. The discovery and function of filaggrin. **International Journal of Molecular Sciences**, v. 23, n. 3, p. 1455, 2022.

39. Thyssen, Jacob P.; Kezic, Sanja. Causes of epidermal filaggrin reduction and their role in the pathogenesis of atopic dermatitis. **Journal of Allergy and Clinical Immunology**, v. 134, n. 4, p. 792-799, 2014.

40. Armengot-Carbo, M.; Hernández-Martín, Á.; Torrelo, A. The role of filaggrin in the skin barrier and disease development. **Actas Dermo-Sifiliográficas** (English Edition), v. 106, n. 2, p. 86-95, 2015.

41. Presland, Richard B. et al. Regulated expression of human filaggrin in keratinocytes results in cytoskeletal disruption, loss of cell–cell adhesion, and cell cycle arrest. **Experimental cell research**, v. 270, n. 2, p. 199-213, 2001.

42. Hovhannisyan, Lilit et al. Excess filaggrin in keratinocytes is removed by extracellular vesicles to prevent premature death and this mechanism can be hijacked by Staphylococcus aureus in a TLR2-dependent fashion. 2022.

43. Omari Shekaftik, Soqrat; Nasirzadeh, Nafiseh. 8-Hydroxy-2′-deoxyguanosine (8- OHdG) as a biomarker of oxidative DNA damage induced by occupational exposure to nanomaterials: A systematic review. **Nanotoxicology**, v. 15, n. 6, p. 850-864, 2021.

44. Kim, Junghyun et al. Methylglyoxal induces cellular damage by increasing argpyrimidine accumulation and oxidative DNA damage in human lens epithelial cells.

Biochemical and biophysical research communications, v. 391, n. 1, p. 346-351, 2010.

45. Donnellan, Leigh et al. Methylglyoxal induces chromosomal instability and mitotic dysfunction in lymphocytes. **Mutagenesis**, v. 36, n. 5, p. 339-348, 2021.

46. Seo, Kyuhwa et al. Resveratrol attenuates methylglyoxal-induced mitochondrial dysfunction and apoptosis by Sestrin2 induction. **Toxicology and applied pharmacology**, v. 280, n. 2, p. 314-322, 2014.

47. Moldogazieva, Nurbubu T. et al. Lipid peroxidation: Reactive carbonyl species, protein/DNA adducts, and signaling switches in oxidative stress and cancer. **Biochemical and Biophysical Research Communications**, v. 687, p. 149167, 2023.

48. Lee, Seon Hwa et al. Lipid peroxidation-derived modification and its effect on the activity of glutathione peroxidase 1. **Free Radical Biology and Medicine**, v. 208, p. 252-259, 2023.

49. López de Padilla, Consuelo M. et al. Picrosirius red staining: revisiting its application to the qualitative and quantitative assessment of collagen type I and type III in tendon. **Journal of Histochemistry & Cytochemistry**, v. 69, n. 10, p. 633-643, 2021.

50. Fisher, Gary J.; Varani, James; Voorhees, John J. Looking older: fibroblast collapse and therapeutic implications. **Archives of dermatology**, v. 144, n. 5, p. 666-672, 2008.

51. Varani, James et al. Decreased collagen production in chronologically aged skin: roles of age-dependent alteration in fibroblast function and defective mechanical stimulation. **The American journal of pathology**, v. 168, n. 6, p. 1861-1868, 2006.

52. Chen CY, Zhang JQ, Li L, Guo MM, He YF, Dong YM, Meng H, Yi F. Advanced Glycation End Products in the Skin: Molecular Mechanisms, Methods of Measurement, and Inhibitory Pathways. **Front Med (Lausanne)**. 2022 May 11;9:837222. doi: 10.3389/fmed.2022.837222. PMID: 35646963; PMCID: PMC9131003.

53. Kritas, S. K. et al. Impact of mast cells on the skin. **International journal of immunopathology and pharmacology**, v. 26, n. 4, p. 855-859, 2013.

54. Church, Martin K.; Clough, Geraldine F. Human skin mast cells: in vitro and in vivo studies. **Annals of Allergy, Asthma & Immunology**, v. 83, n. 5, p. 471-475, 1999.

55. Theoharides, Theoharis C. et al. Mast cells and inflammation. **Biochimica et Biophysica Acta (BBA)-Molecular Basis of Disease**, v. 1822, n. 1, p. 21-33, 2012.

56. Voss, Martin et al. Mast cells in the skin: defenders of integrity or offenders in inflammation?. **International Journal of Molecular Sciences**, v. 22, n. 9, p. 4589, 2021.

57. Bentov, Itay; Reed, May J. The effect of aging on the cutaneous

microvasculature. **Microvascular research**, v. 100, p. 25-31, 2015.

58. Russell, Nicola S. et al. Blood and lymphatic microvessel damage in irradiated human skin: The role of TGF-β, endoglin and macrophages. **Radiotherapy and Oncology**, v. 116, n. 3, p. 455-461, 2015.

59. Ryan, Terence. The ageing of the blood supply and the lymphatic drainage of the skin. **Micron**, v. 35, n. 3, p. 161-171, 2004.

60. Lechner, Anna et al. Comparing skin characteristics and molecular markers of xerotic foot skin between diabetic and non-diabetic subjects: An exploratory study. **Journal of tissue viability**, v. 28, n. 4, p. 200-209, 2019.

61. Rawlings, A.V.; Harding, C. R. Moisturization and skin barrier function. **Dermatologic therapy**, v. 17, p. 43-48, 2004.

62. Lintzeri, D. A. et al. Epidermal thickness in healthy humans: a systematic review and meta-analysis. **Journal of the European Academy of Dermatology and Venereology**, v. 36, n. 8, p. 1191-1200, 2022.

63. Ferrara, Francesca et al. Inflammasome activation in pollution-induced skin conditions. **Plastic and reconstructive surgery**, v. 147, n. 1S-2, p. 15S-24S, 2021.

64. Jiménez-Vidal, Luisa et al. Nuclear factor erythroid 2–related factor 2 and its relationship with cellular response in nickel exposure: A systems biology analysis. **BMC Pharmacology and Toxicology**, v. 20, p. 1-13, 2019.

65. Portt, Liam et al. Anti-apoptosis and cell survival: a review. **Biochimica et Biophysica Acta (BBA)-Molecular Cell Research**, v. 1813, n. 1, p. 238-259, 2011.

2. Anti-inflammatory and antioxidant activities of *Commiphora leptophloeos* leaf and bark extracts in skin ex vivo experiments

Caroline Tomaz Massardi[1], Eduarda Pires Costa[1], Mônica Morais Santos[2], Allan Rodrigues Pires[1], Manoela Maciel dos Santos Dias[2], Rosinea Aparecida de Paula[2], Marcos V. de Sousa Pereira[3], Jemmyson R. de Jesus[3], Silvana Maria Zucolotto Langassner[4,] Reggiani Vilela Gonçalves*[2,5]

[1] Department of General Biology, Federal University of Viçosa, Peter Henry Rolfs Ave, s/n, University Campus, Viçosa, MG, 36570-900, Brazil; caroline.massardi@ufv.br; eduarda.costa@ufv.br; allan.pires@ufv.br

[2] Department of Animal Biology, Federal University of Viçosa, Peter Henry Rolfs Ave, s/n, University Campus, Viçosa, MG, 36570-900, Brazil; monica.morais@ufv.br; manoela.santos@ufv.br; rosinea.paula@ufv.br; reggiani.goncalves@ufv.br

[3]Research Laboratory in bionanomaterials, LPbio, Department of Chemistry, Federal University of Viçosa, 36570-900, Viçosa, Minas Gerais, Brazil.

[4]Department of Pharmaceutical Sciences, Faculty of Pharmacy, Federal University of Rio Grande do Norte, 59012-570, Natal, Brazil; szucolotto@hotmail.com (SMZL).

[5] Department of Animal Sciences, Plants for Human Health Institute, North Carolina State University, Kannapolis, NC 28081, USA; rvilela@ncsu.edu

*Corresponding author: Reggiani Vilela Gonçalves; rvilela@ncsu.edu / reggiani.goncalves@ufv.br

Abstract

The skin serves as the primary protective barrier of the body against various external harmful agents, such as pollution and ultraviolet (UVA and UVB) radiation. When intact and functional, this barrier contributes to the maintenance of systemic homeostasis in the face of daily challenges. However, exposure to stressors—whether internal or external—can trigger a process known as oxi-inflammation. This phenomenon is characterized by a positive feedback

loop between oxidative stress and inflammation, leading to a sustained cycle of tissue damage. Among the known stress-inducing agents, methylglyoxal stands out as a reactive compound capable of disrupting biochemical balance, thereby promoting oxi-inflammatory conditions. In this context, the search for natural products that support cutaneous homeostasis has gained increasing attention, particularly those derived from plants used in traditional medicine. In line with this aim, the present study investigated the efficacy of leaf and bark extracts of *Commiphora leptophloeos*—a species native to the northeastern Brazilian caatinga and widely recognized for its anti-inflammatory and antioxidant properties—under methylglyoxal-induced stress. Two concentrations of each plant part were tested: leaves at 350 and 500 µg/mL, and bark at 50 and 100 µg/mL, using an ex vivo experimental model. Analyses included the quantification of antioxidant enzymes and oxidative stress markers, histopathological and immunohistochemical evaluations, PCR, and skin permeation assays. The results demonstrated that *C. leptophloeos* extracts exert multifaceted effects on tissue undergoing oxi-inflammation. The leaf extract at 500 µg/mL and the bark extract at 100 µg/mL showed the most pronounced anti-inflammatory activity, while the leaf extract at 500 µg/mL and the bark extracts at 50 and 100 µg/mL exhibited superior antioxidant effects. Overall, the leaf extract at 500 µg/mL emerged as the most effective in protecting skin tissue from oxidative and glycative stress.

Keywords: *Commiphora leptophloeos, ex vivo,* oxi-inflammation, methylglyoxal, antioxidant

2.1. Introduction

The skin is our primary interface with the external environment. As such a vital barrier, healthy skin provides a more effective defense against daily external challenges, contributing to the maintenance of overall physiological homeostasis (Dehkordi et al., 2019). In addition to exogenous stressors, the body also produces endogenous ones, which can negatively affect skin health by triggering inflammation and oxidative stress (Majtan et al., 2021).

A key process involved in this imbalance is OxInflammation, defined as the interactive outcome of oxidative stress and inflammation in a self-sustaining positive feedback loop (Chiarello et al., 2023; Sharma et al., 2022; Fraile-Ramos et al.,2023). Oxidative stress arises when the equilibrium between oxidant molecules—mainly reactive oxygen species (ROS)—and antioxidant defenses shifts in favor of the oxidants. ROS are capable of activating transcription factors such as NF-κB, thereby initiating inflammatory signaling pathways. In

turn, these inflammatory responses promote the release of cytokines and other mediators that further stimulate ROS production, exacerbating oxidative stress (Valacchi et al., 2016).

Among the exogenous stressors implicated in this process, methylglyoxal (MG) stands out as a particularly potent agent. MG is a highly reactive byproduct of glucose metabolism, and is also present in the environmental sources such as cigarette smoke, rainwater, and various food products. It readily interacts with proteins and other biomolecules, forming advanced glycation end-products (AGEs), which bind to RAGEs (receptors for AGEs) expressed on multiple cell types, triggering diverse pathological processes (Sartori & Berchara, 2010). The accumulation of AGEs further amplifies inflammation by inducing the expression of pro-inflammatory cytokines, intensifying oxidative stress in a vicious cycle (Desai et al., 2010). Given its high reactivity and well-documented capacity to disrupt redox homeostasis (Wang et al., 2022; Sugiura et al., 2021), MG was selected as the cellular stressor in this study.

In alignment with global efforts to reduce and ultimately replace the use of animal models in pharmacological research, this study employed an *ex vivo* methodology, which has garnered increasing recognition for its ability to preserve key physiological and biochemical characteristics of native tissue (Neil et al., 2022). This approach involves the use of small fragments of human skin obtained from elective surgeries, maintained in culture media under controlled conditions to enable the evaluation of therapeutic interventions in a context that closely mimics *in vivo* physiology.

In the context of searching for natural compounds capable of supporting skin tissue homeostasis, *Commiphora leptophloeos* - a plant endemic to the Caatinga biome in northeastern Brazil (De Melo Alcântara et al., 2023) - was selected as the focus of investigation os this study. In traditional medicine, extracts from the leaves and bark of this plant have been used to treat inflammatory disorders , edema, infections, and related ailments (Dantas-Medeiros et al., 2021). However, despite its relevance, studies involving *Commiphora leptophloeos* extracts have so far been limited to *in vivo* and *in vitro* models. This approach provided an opportunity to evaluate its effects in a more physiologically relevant ex vivo model, using human biological tissue — which directly represents the potential target of any pharmaceutical or cosmetic formulations developed from the extracts.

Accordingly, the present study aims to evaluate the anti-inflammatory and antioxidant properties of two concentrations of *C. leptophloeos* leaf extract—L350 and L500 (350 and 500 µg/mL, respectively)—and two concentrations of bark extract—B50 and B100 (50 and 100 µg/mL, respectively)—in human skin biopsies subjected to oxidative stress induced by 650 µM of methylglyoxal, a concentration previously validated by our research group with the

ability to generate oxidative and inflammatory damage, without causing loss of cellular predictions (results not yet published). This investigation aims to expand the pharmacological understanding of *C. leptophloeos* while contributing to the development of alternative models in dermatological research.

2.2. Materials and Methods

2.2.1. Plant Material Collection

The bark and leaves of *Commiphora leptophloeos* (Mart.) J.B. Gillett were collected in July 2019 from the rural community of Carao, located in the municipality of Altinho, Pernambuco, Brazil (geographic coordinates: 8°29′32″S, 36°03′03″W). Botanical identification was carried out at the Geraldo Mariz Herbarium of the Federal University of Pernambuco (UFPE), where the specimen was cataloged under the number 46,191. The collection was authorized by the Biodiversity Authorization and Information System (SISBIO), under process number 35017. The scientific research involving this plant material was registered and approved by the National System for the Management of Genetic Heritage and Associated Traditional Knowledge (SISGEN), under registration number A618873.

2.2.2. Preparation of Hydroethanolic Extracts

The collected bark and leaf samples were dried in a forced-air circulation oven at 45 °C and subsequently ground using a knife mill. For each plant part, 200 grams of powdered material were weighed and subjected to static maceration in a hydroethanolic solution (ethanol:water, 70:30 v/v) at a plant-to-solvent ratio of 1:10 (w/v) for 48 hours (first extraction). After this period, the extracts were filtered through Whatman™ No. 1 filter paper. The remaining plant residue was then re-extracted (second extraction) under the same conditions to maximize yield. The two resulting extracts (first and second) were combined and concentrated under reduced pressure using a rotary evaporator (Buchi, Model V-700, Altendorfer Str. 3, Essen, Germany), keeping the temperature below 35 °C to ensure the removal of organic solvents. The concentrated extract was then frozen and lyophilized under a pressure of 200 mT at –20 °C for 72 hours (Model 101, Liotop®, São Carlos, São Paulo, Brazil).

This process yielded 13.0 g (6.5%) of leaf extract and 25.6 g (12.8%) of bark extract.

2.2.3. Sample Preparation

For phytochemical analysis, the leaf and bark extracts of *Commiphora leptophloeos* were subjected to solid-phase extraction (SPE) pre-treatment using Chromabond® cartridges (45 µm, 500 mg, 6 mL), followed by drying under a nitrogen (N_2) atmosphere, according to a protocol adapted from Dantas-Medeiros et al. (2021).

For the pharmacological activity assays, stock solutions of bark extracts (50 and 100 µg/mL) and leaf extracts (350 and 500 µg/mL) were prepared based on previously established protocols for use in ex vivo experiments. These concentrations were chosen from previous studies (unpublished data).

To ensure consistency in terminology throughout this study, the bark extracts were designated as B50 and B100, corresponding to concentrations of 50 and 100 µg/mL, respectively, and the leaf extracts were labeled as L350 and L500, referring to concentrations of 350 and 500 µg/mL.

2.2.4. Phytochemical Characterization of *Commiphora leptophloeos* Extracts

The phytochemical analysis of the leaf and bark extracts of *Commiphora leptophloeos* was performed using sequential mass spectrometry with an ion trap, employing electrospray ionization and direct flow injection (FIA-ESI-IT-MS/MS) (Thermo Scientific®, San Jose, California, USA), according to the methodology described by Dantas-Medeiros et al. (2021).

For the analyses, the extracts were diluted in absolute methanol to a final concentration of 10 ppm. The operational parameters included: ion source temperature of 280 °C, spray voltage of 5.00 kV, capillary voltage of -47 V, tube lens voltage of -226 V, pump flow rate of 5.0 µL/min, with negative ionization mode. The analysis range was set between m/z 100 and 2000, performing full scan acquisition for MS spectra. Subsequently, MS/MS spectra were obtained for selected precursor ions using collision-induced dissociation (CID) with a collision energy of 30 V. Data acquisition and processing were conducted using Xcalibur™ software version 1.3 (Thermo Scientific®).

2.2.5. Quantification of Total Phenolic Content (TPC) and Total Flavonoid Content (TFC)

The total phenolic content (TPC) was quantified using the Folin-Ciocalteu method, as described by Dantas-Medeiros et al. (2021). Solutions of each dry extract (leaves and bark)

were prepared at a concentration of 2 mg/mL, and 25 µL of each solution was added to a 96-well plate. To each well, 125 µL of Folin-Ciocalteu reagent (v/v) and 100 µL of 7.5% Na_2CO_3 solution were added. The samples were incubated at 25 ± 2°C for 30 minutes, protected from light. Absorbance was measured using an ELISA microplate reader at 765 nm. The phenolic content was calculated based on a gallic acid (GAE) calibration curve (R^2 = 0.9925) and expressed as milligrams of gallic acid equivalents per gram of extract (mg GAE/g extract).

The total flavonoid content (TFC) was determined using the aluminum chloride method, as described by Da Silva et al. (2024), with a quercetin (QE) standard curve (R^2 = 0.9903). Absorbance readings were performed on a spectrophotometer at 415 nm. The results were expressed as milligrams of quercetin equivalents per gram of extract (mg QE/g extract). All experiments were performed in triplicate, with three independent biological samples (n = 9).

2.2.6. Ex Vivo Analysis with Human Skin Biopsies

For this study, we collected human skin biopsies donated from elective surgeries performed at a local hospital in Viçosa, Minas Gerais. Approval was obtained from the Ethics Committee on Human Research (CEP) of the Federal University of Viçosa (approval number 82329224.7.0000.5153) for the collection and experimental procedures. The biopsies, measuring 12 mm in diameter, were processed by removing the subcutaneous adipose tissue using a scalpel and then washed with phosphate-buffered saline (PBS).

Following these initial procedures, the biopsies were placed in six-well plates containing Dulbecco's Modified Eagle Medium (DMEM) with high glucose (GIBCO, USA), supplemented with 1% fetal bovine serum (FBS; GIBCO, USA), 2.5 µg/mL amphotericin B, and 1% liquid penicillin. The plates were incubated for 24 hours at 37°C with 5% CO2 to allow for recovery and acclimatization (Ferrara et al., 2020).

After this incubation period, the medium was supplemented with the stressor methylglyoxal at a concentration of 650 µM. The methyl concentration was determined in a previous study (unpublished data - submitted for review). Leaf extracts of *Commiphora leptophloeos* were applied at concentrations of 350 and 500 µg/mL, and bark extracts at concentrations of 50 and 100 µg/mL. In addition, biopsies were maintained as negative controls, containing DMEM without methylglyoxal, and as positive controls, containing DMEM with methylglyoxal but no extract treatment. The biopsies received the respective treatments for seven consecutive days, with culture media being renewed daily.

2.2.7. Antioxidant Enzyme Activities and Oxidative Stress Markers

To assess the activity of antioxidant enzymes and oxidative stress markers, the designated skin biopsy fragments were collected after seven days of treatment, immediately frozen in liquid nitrogen (-196 °C), and stored in an ultrafreezer (-80°C). The samples were manually macerated using a pestle in the presence of an EDTA buffer (0.2 mol/L phosphate buffer, 1 mmol/L ethylenediaminetetraacetic acid, pH 7.4), then centrifuged at 15.000 g for 10 minutes at 4°C. The supernatant was separated for the analysis of antioxidant enzyme activities, including catalase (CAT), superoxide dismutase (SOD), and glutathione S-transferase (GST), while the pellet was used for the analysis of carbonylated proteins (PC).

SOD activity was measured following the protocol described by Dieterich et al. (2000), which is based on the reduction of the auto-oxidation of pyrogallol.

CAT activity was determined using the method proposed by Aebi (1984), in which enzyme activity is defined by its ability to decompose hydrogen peroxide into water and oxygen.

For GST activity, we followed the method described by Habig et al. (1981), which measures the enzyme's ability to metabolize 1-chloro-2,4-dinitrobenzene (CDNB) conjugated with reduced glutathione.

Lastly, the analysis of carbonylated proteins was performed according to the protocol described by Levine (1990), which quantifies the amount of carbonylated proteins in the sample. To normalize the results, the total protein content in the supernatant was measured using the Bradford reagent.

2.2.8. Explant preparation

The biopsies designated for histopathological and immunohistochemistry assays were collected after seven days of treatment and fixed in 10% formalin overnight, following the protocol described by Morais-Santos et al. (2018). The following day, the samples were washed in PBS, dehydrated through a series of ethanol concentrations, cleared with xylene and embedded in paraffin for further processing. The paraffin blocks containing the biopsies were sectioned using a Leica Multicut 2045 microtome (Reichert-Jung Products, Germany), obtaining 5 μm thick tissue sections. The sections intended for immunohistochemical analysis were placed on silanized slides, while those for histological assays were placed on standard glass slides.

2.2.8.1. Histological Analysis

In the histological assays, we evaluated and quantified mast cells (Churukian & Schenk, 1981), blood vessels (Gonçalves et al., 2010), and type III and type I collagen fibers (Cupertino et al., 2013). All slides were deparaffinized in a series of xylene gradients and rehydrated with ethanol before being subjected to specific staining procedures.

For this analysis, mast cells were identified using toluidine blue staining, while blood vessels were visualized through hematoxylin and eosin (H&E) staining. Type III and type I collagen fibers were analyzed using Sirius Red staining. Following the staining procedures, the slides were rehydrated, mounted with coverslips, and prepared for microscopic analysis.

2.2.8.2. Immunohistochemical Analysis

Immunohistochemical analyses were conducted to evaluate the effectiveness of the extracts in protecting the tissue samples from the damage induced by methylglyoxal (MG), using markers of skin integrity and oxidative stress, as outlined in the protocol established by Morais-Santos et al. (2018). Tissue sections (5 μm) were deparaffinized, rehydrated, and washed in phosphate-buffered saline (PBS), followed by blocking of endogenous peroxidase to prevent nonspecific background staining. Antigen retrieval was performed using heat-induced epitope retrieval (HIER) in 0.1 M sodium citrate buffer (pH 6.0) in a microwave oven for 20 minutes.

To block nonspecific binding, the sections were incubated with 5% bovine serum albumin (BSA) for 1 hour. After the BSA solution was removed, primary antibodies were applied: anti-catalase (mouse or rabbit, 1:50, sc-271803), anti-filaggrin (mouse or rabbit, 1:250, sc-66192), anti-8OHdG (mouse or rabbit, 1:250, sc-393871), and anti-4HNE (goat, 1:50, AB5605). Incubation was carried out overnight at 4°C in a humid chamber. Negative controls were prepared by substituting the primary antibodies with PBS to validate the specificity of the immunostaining.

Following incubation with the primary antibodies, the sections were treated with secondary antibodies conjugated to horseradish peroxidase (HRP) as specified by the manufacturer, for 1 hour at room temperature. Immunoreactivity was visualized using a chromogenic solution containing 0.05% diaminobenzidine tetrahydrochloride (DAB) and 0.01% hydrogen peroxide

in 0.05 M Tris-HCl buffer (pH 7.4). Finally, the slides were counterstained with Harris hematoxylin for nuclear contrast.

2.2.8.3. Analysis of Histological and Immunohistochemical Sections

For both methodologies, images were captured using a photomicroscope (EVOS™ M5000 Imaging System from Thermo Fisher Scientific) coupled with a digital camera (3® -QColor Olympus) at a magnification of 40x. Ten images per sample were taken and analyzed using the Image-Pro Plus 4.5 imaging software (Media Cybernetics, Silver Spring, USA), with a grid of 300 points for counting the structures of interest.

2.2.9. RNA Extraction and Quantitative Reverse Transcription PCR (RT-qPCR)

RNA extraction from human skin biopsies was performed using TRIzol™ reagent (Invitrogen, ThermoFisher Scientific, Waltham, MA, USA). Briefly, skin samples were placed in microtubes containing 1 mL of TRIzol, and the tissues were homogenized using an Omni International sample homogenizer (Tissue Master 125). Then, 140 µL of RNase-free chloroform was added to each microtube, followed by centrifugation for 15 minutes at 12,000 x g at 4°C. The aqueous phase containing RNA was transferred to a new tube, and the chloroform extraction step was repeated. RNA precipitation was performed by adding 500 µL of RNase-free isopropanol and centrifuging at 12,000 x g at 4°C for 30 minutes. The RNA pellet was washed three times with 75% ethanol and centrifuged at 10,000 x g at 4°C for 10 minutes. The pellet was then resuspended in 20 µL of nuclease-free water and quantified using a Multiskan SkyHigh spectrophotometer (Thermo Fisher Scientific, Waltham, MA, USA).

Subsequently, 1 µg of total RNA from each sample was reverse-transcribed into complementary DNA (cDNA) using the High Capacity cDNA Reverse Transcription Kit (Thermo Fisher Scientific, Waltham, MA, USA), following the manufacturer's protocol. The mRNA levels of TLR-4, NF-kB, COX2, NRF-2, and HO-1 were analyzed by quantitative real-time PCR (qPCR) using the PowerTrack™ SYBR™ Green Master Mix (Thermo Fisher Scientific, Waltham, MA, USA) on a QuantStudio™ 3 Real-Time PCR System (Thermo Fisher Scientific, Waltham, MA, USA), according to the manufacturer's guidelines. Gene expression was quantified based on the number of cycles required to reach a predefined threshold value (Ct value) for each sample, with glyceraldehyde 3-phosphate dehydrogenase

(GAPDH) used as the housekeeping gene. After normalization, the fold change was determined using the relative standard curve method.

The specific primers sequences are presented in Table 1.

Table 1. Genes and primer sequences used.

Gene	**Sequence 5'- 3'**	**References**
TLR-4 Human	F. TGG TGT CCC AGC ACT TCA TC R. GCC AGG TCT GAG CAA TCT CAT A	Dias, M., M., S. et al. 2015
NF-kB Human	F-TGG GAA TGG TGA GGT CAC TCT R- TCC TGA ACT CCA GCA CTC TCT TC	Dias, M., M.. S. et al. 2014
COX-2 Human	F-AGG GTT GCT GGT GGT AGG AA R- GGT CAA TGG AAG CCT GTG ATA CT	Dias, M., M., S. et al. 2014
NRF-2 Human	F-TTC CCG GTC ACA TCG AGA G R- TCC TGT TGC ATA CCG TCT AAA TC	Golpour et al., 2020
HO-1 Human	F-TCC GAT GGG TCC TTA CAC TC R- TAA GGA AGC CAG CCA AGA GA	Min et al., 2022
GAPDH Human	F-TCG GAG TCA ACG GAT TTG GT R- TTC CCG TTC TCA GCC TTG AC	Ivarsson et al., 2023

2.3. Skin Permeation

The evaluation of permeation through a biological barrier was conducted using a Franz diffusion cell with human skin biopsies as the membrane (n = 2), following a methodology adapted from Andrade et al. (2024). The skin was properly prepared and adjusted to fit the shape of the diffusion cell. In the donor compartments, 1 mL of leaf (350 and 500 µg/mL) and

bark (50, and 100 µg/mL) extracts was applied onto the skin surface. As the receptor phase, a phosphate-buffered saline (PBS) solution with pH 7.4 was used. The assay was conducted at a controlled temperature of 37.0 ± 0.5 °C for a period of 24 hours. After this period, the different layers of the skin were separated to evaluate the retention of the compound. The extract from the stratum corneum was removed using the tape-stripping technique. The epidermis was separated after immersion in deionized water at 60°C for 45 seconds, followed by scraping with a scalpel. The remaining dermal tissue was cut into cubes. Each layer was placed in tubes containing acetonitrile, subjected to vigorous vortex shaking for 2 minutes, and then treated in an ultrasonic bath for 30 minutes. The obtained samples were quantified by UV/Vis spectrophotometry at λ = 197 nm (Leaf) and λ = 195 nm (Bark), using analytical calibration curves with standard concentrations ranging from 0.006 to 1.000 µg/mL (Bark) and 0.006 to 0.700 µg/mL (Leaf).

2.3.1. Statistical Analyses

Statistical analyses were performed using GraphPad Prism 8 software (GraphPad Software Inc., Boston, MA, USA). Results are expressed as mean ± standard deviation (SD). Data distribution was assessed using the Kolmogorov-Smirnov test. For normally distributed (parametric) data, group comparisons were made using one-way analysis of variance (ANOVA) followed by Tukey's post hoc test. For non-parametric data, the Kruskal-Wallis test was applied. A p-value of less than 0.05 was considered statistically significant.

2.4. Results

2.4.1. Antioxidant Enzyme Activities and Oxidative Stress Markers

Oxidative stress assays were performed to assess the potential antioxidant activity of *Commiphora leptophloeos* leaf and bark extracts. In the analysis of SOD activity, it was observed that the bark extracts at concentrations of 50 and 100 µg/mL maintained enzymatic activity similar to the negative control parameters. On the other hand, the concentrations of 350 and 500 µg/mL of leaf extract showed an increase in SOD activity, with the 350 µg/mL concentration being even higher than the positive control. CAT activity differed from both the positive and negative controls at all concentrations of leaf and bark extracts, with the lowest enzymatic activity observed at B50 and the highest at L350. For glutathione-S-transferase activity, the two concentrations of leaf extract maintained activity similar to the positive

control, while the two concentrations of bark extract indicated higher levels of enzymatic activity. All extracts reduced carbonylated proteins levels compared to the positive control.

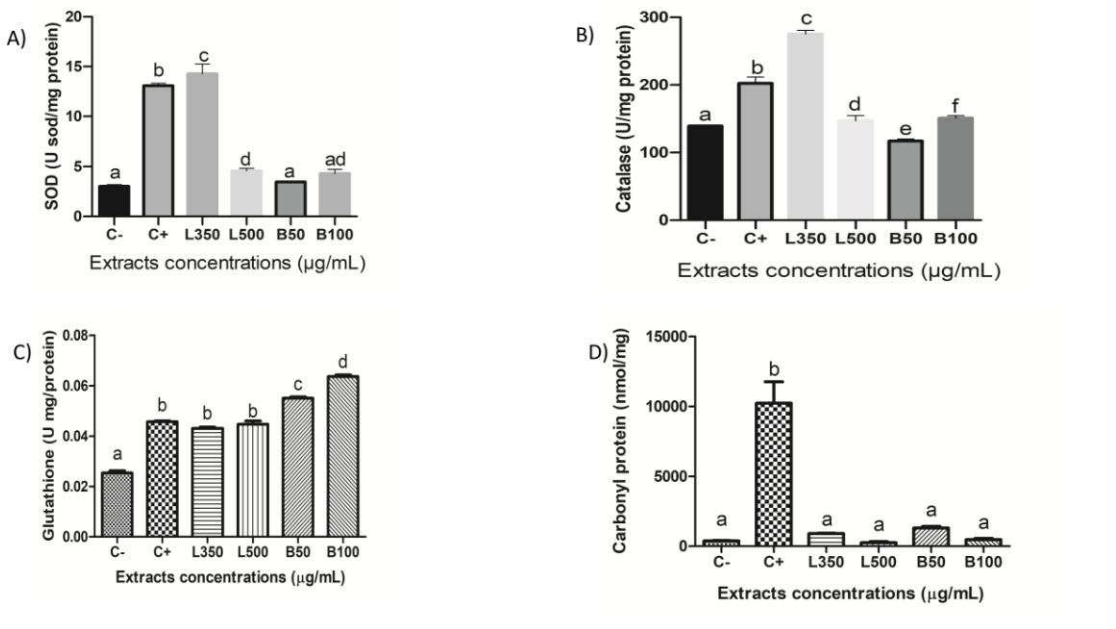

Figure 1. Effects of *Commiphora leptophloeos* bark and leaf extracts, administered at different concentrations on ex vivo skin samples, on oxidative stress biomarkers and antioxidant enzymes. (A) Superoxide dismutase enzyme activity, (B) catalase enzyme activity, (C) glutathione-S-transferase activity, and (D) carbonylated protein concentration. C- refers to skin not exposed to methylglyoxal; C+ refers to skin exposed only to methylglyoxal at a concentration of 650 µM without treatment with extracts. B50, B100, L350 and L500, , refers to skin exposed to methylglyoxal and treated with bark (50 and 100 µg/mL) and leaf (350 and 500µg/mL) extracts of *Commiphora leptophloeos*.According to the Tukey test, means indicated with different letters show statistically significant differences ($p<0.05$).

2.4.2. Histological Assays.

In the histological analyses, no alterations were observed in the quantification of mast cells at any concentration of the extracts compared to the positive and negative controls.

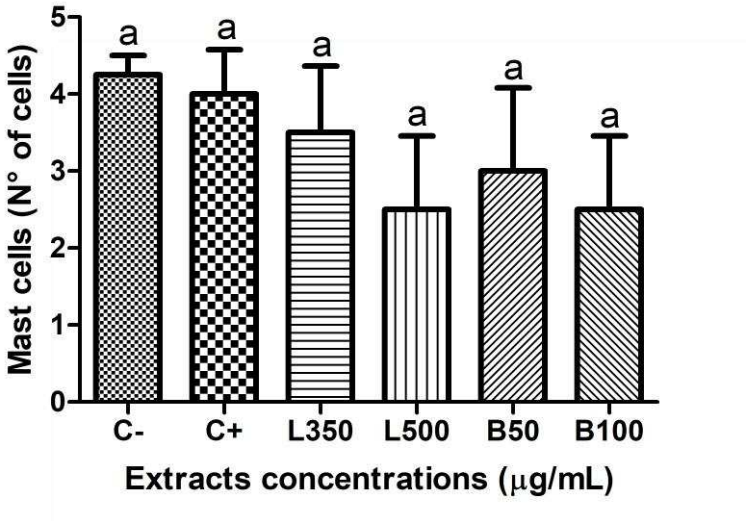

Figure 2. Proportion of mast cell in skin samples treated with bark and leaves extracts of *Commiphora leptophloeos* at different concentrations evaluated histologically. C-: tissues not exposed to methylglyoxal; C+: tissues exposed only to methylglyoxal at a concentration of 650 µM. L350, L500, B50, and B100: tissues exposed to methylglyoxal and treated with leaf (350 and 500µg/mL) and bark extracts (50, and 100 µg/mL) of *Commiphora leptophloeos*. According to Tukey's test, means with the same letter do not show statistically significant differences ($p>0.05$).

The quantification of blood vessels in the samples also did not reveal any significant differences between the extracts and the negative control, maintaining lower levels of angiogenesis compared to the positive control. The concentration of B100 was the one that showed the lowest levels.

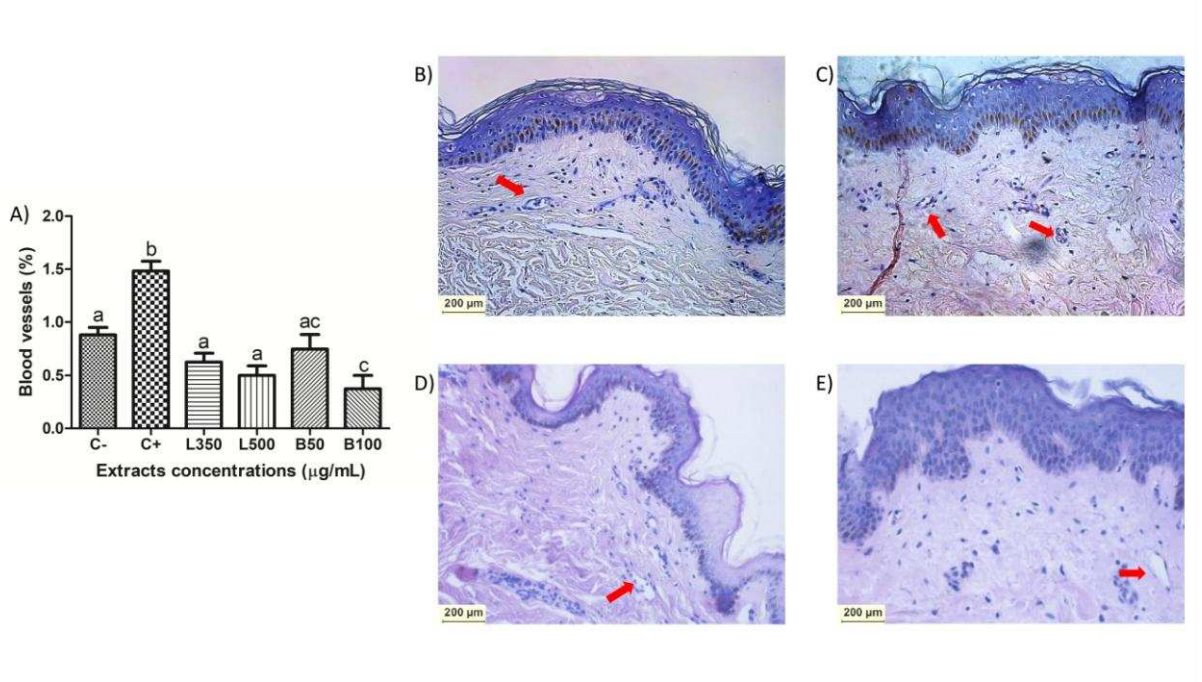

Figure 3. Analysis of blood vessels in skin samples exposed to methylglyoxal and treated with leaf and bark extracts of *Commiphora leptophloeos*. (A) Percentage of blood vessels. (B) Photomicrograph of skin of negative control - tissues not exposed to methylglyoxal; (C) Photomicrograph of skin of positive control - exposed only to methylglyoxal at a concentration of 650 µM; (D) skis exposed to methylglyoxal and treated with bark extracts at a concentration of 50 µg/mL; (F) skin fragments exposed to methylglyoxal and treated with bark extracts at a concentration of 100 µg/mL. The skins were stained with hematoxylin and eosin (H&E). According to the Tukey test, means with different letters show statistically significant differences ($p<0.05$). Red arrowheads indicate blood vessels. Scale bar = 200 µm

Analysis of dermal structural proteins showed a reduction of type III collagen in all treatments, compared to negative control, and a reduction of type I collagen in all treatments, compared with negative and positive controls. The reduction in type III collagen was less pronounced in the two concentrations of bark extract tested. In contrast, for type I collagen, the concentrations that exhibited a less pronounced reduction were L500 and B50.

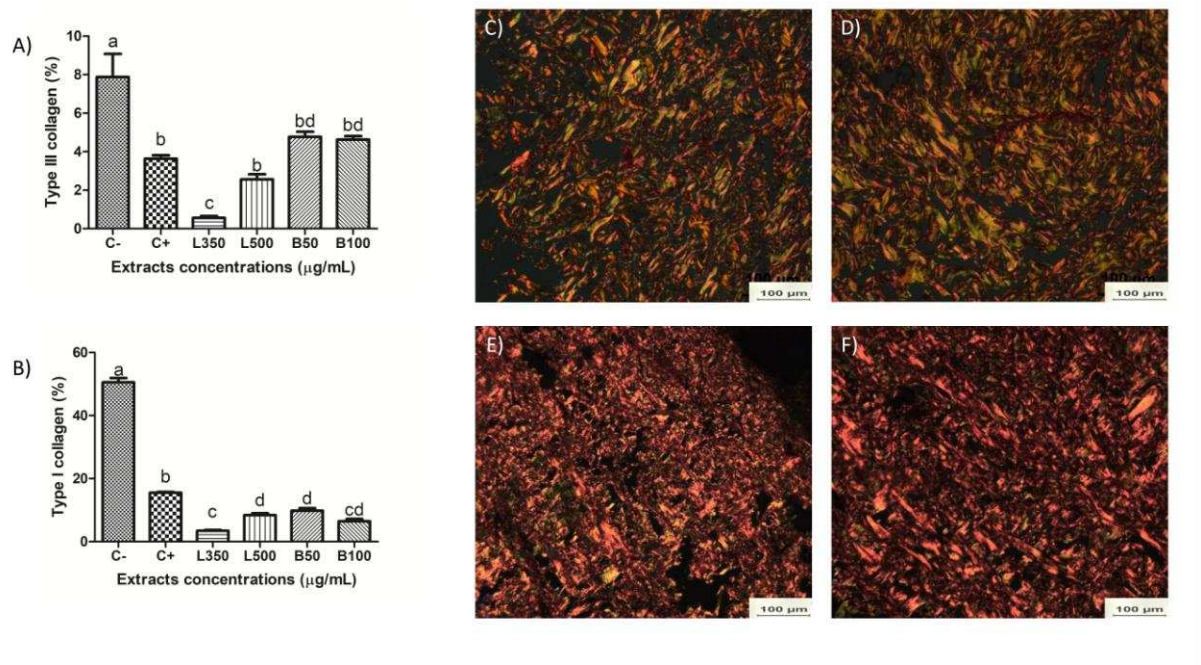

Figure 4. (A) Proportion of type III collagen and (B) type I collagen in skin samples exposed to methylglyoxal and treated with leaf and bark extracts of *Commiphora leptophloeos*. C-: skin fragments without exposure to methylglyoxal (culture medium only); C+: fragments exposed to methylglyoxal at a concentration of 650 µM; L350, L500, B50, and B100: tissues exposed to methylglyoxal and treated with leaf (350 and 500 µg/mL) and bark extracts (50, and 100 µg/mL) of *Commiphora leptophloeos*. According to the Tukey test, means with different letters exhibit statistically significant differences ($p<0.05$).

(C, D, E and F) Representative photomicrographs obtained by polarized microscopy of samples stained with Sirius Red. (C) Negative control; (D) Positive control; (E) skin fragments exposed to methylglyoxal and treated with leaf extracts at a concentration of 350 µg/mL; (F) skin fragments exposed to methylglyoxal and treated with bark extracts at a concentration of 50 µg/mL. Green shades indicate the presence of type III collagen (reticular fibers), while red to yellow shades indicate type I collagen. Scale bar = 100 µm

2.4.3. Immunohistochemical Assay

In the immunohistochemical assays, we observed a reduction in filaggrin protein levels in all concentrations of bark and leaf extracts tested, when compared to the positive controls.

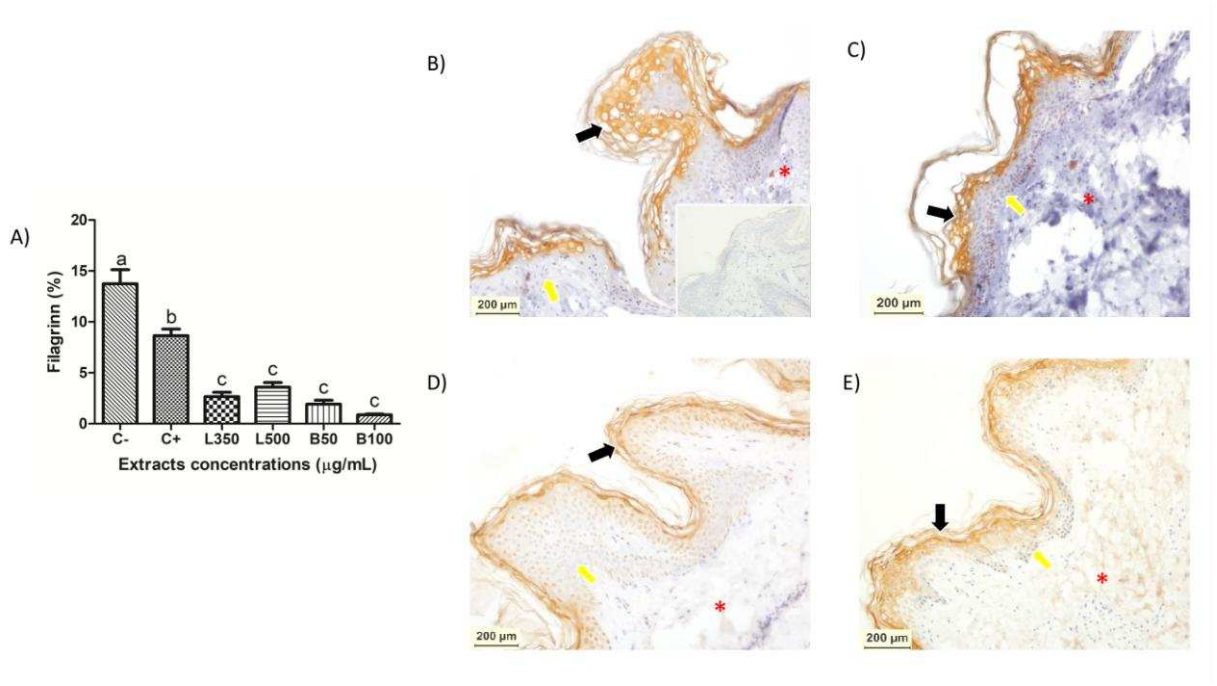

Figure 5. (A) Proportion of filaggrin evidenced by immunostaining in ex vivo skin fragments exposed to methylglyoxal and treated with leaf and bark extracts of *Commiphora leptophloeos*. (B, C and D) Representative photomicrograph of filaggrin immunostaining of skin. C-: skin fragments not exposed to methylglyoxal (culture medium only); C+: skin fragments exposed to methylglyoxal at a concentration of 650 µM; L350, L500, B50, and B100: tissues exposed to methylglyoxal and treated with leaf (350 and 500µg/mL) and bark extracts (50, and 100 µg/mL) of *Commiphora leptophloeos*. According to the Tukey test, means with different letters exhibit statistically significant differences ($p<0.05$). (B) skin fragments not exposed to methylglyoxal, (C) skin fragments exposed to methylglyoxal at concentrations of 650 µM, (D) skin fragments exposed to methylglyoxal and treated with leaf extract at 350 µg/mL, (E) skin fragments exposed to methylglyoxal and treated with bark extract at 50 µg/mL. Black arrows indicate fillagrin, yellow arrows indicate epidermis and red asterisks indicate dermis. Scale bar = 200 µm.

In catalase immunostaining, we observed reduced catalase levels for most extract concentrations tested, except for B50, when compared to the positive control.

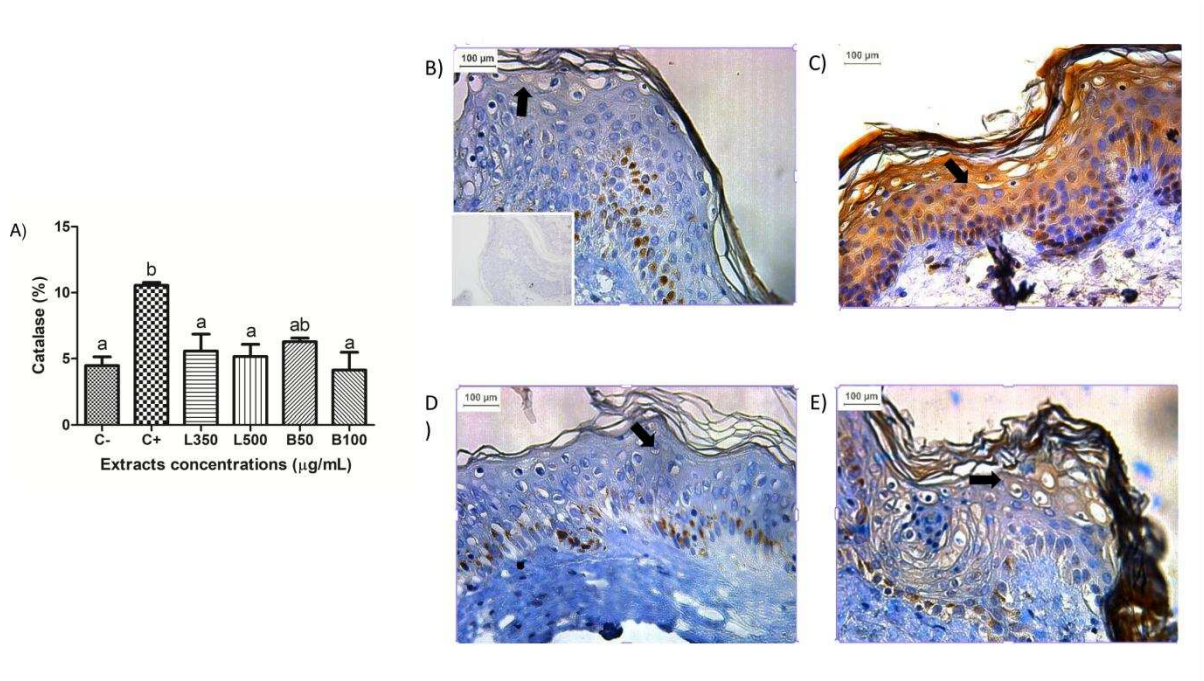

Figure 6. (A) Proportion of catalase evidenced by immunostaining in ex vivo skin fragments exposed to methylglyoxal and treated with leaf and bark extracts of *Commiphora leptophloeos*. C- *s*kin fragments not exposed to methylglyoxal (culture medium only); C+: skin fragments exposed to methylglyoxal at a concentration of 650 µM; L350, L500, B50, and B100: tissues exposed to methylglyoxal and treated with leaf (350 and 500µg/mL) and bark extracts (50, and 100 µg/mL) of *Commiphora leptophloeos*. According to the Tukey test, groups with different letters exhibit statistically significant differences ($p<0.05$). (B, C, D and E) Representative photomicrograph of catalase immunostaining of skin. (B) skin fragments not exposed to methylglyoxal, (C) skin fragments exposed to methylglyoxal at concentrations of 650 µM, (D) skin fragments exposed to methylglyoxal and treated with leaf extract at 350 µg/mL, (E) skin fragments exposed to methylglyoxal and treated with bark extract at 50 µg/mL. Black arrows indicate immunohistochemical signal for catalase in the epidermis. Scale bar = 100 µm.

All treatments reduced the 8 OHdG immunostaining levels compared to the positive control, except for the treatment L350.

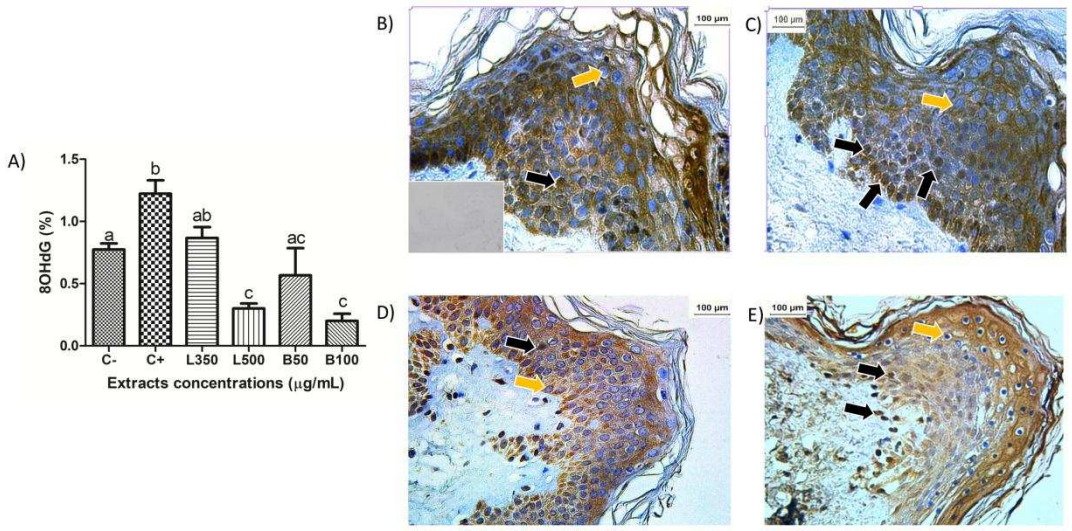

Figure 7. (A) Proportion of 8OHdG evidenced by immunostaining in ex vivo skin fragments exposed to methylglyoxal and treated with leaf and bark extracts of *Commiphora leptophloeos*. C-: skin fragments not exposed to methylglyoxal (culture medium only); C+: skin fragments exposed to methylglyoxal at a concentration of 650 µM; L350, L500, B50, and B100: tissues exposed to methylglyoxal and treated with leaf (350 and 500µg/mL) and bark extracts (50, and 100 µg/mL) of *Commiphora leptophloeos*. According to the Tukey test, means with different letters exhibit statistically significant differences ($p<0.05$). Photomicrograph of epithelial tissue with immunohistochemical staining for 8 OHdG and hematoxylin staining. Control group = Skin fragments not exposed to methylglyoxal (B), skin fragments exposed to methylglyoxal at concentrations of 650 µM (C), skin fragments exposed to methylglyoxal and treated with leaf extract at 500 µg/mL (D), skin fragments exposed to methylglyoxal and treated with bark extract at 50 µg/mL (E). Black arrows indicate immunostained cell nuclei. Yellow arrowheads indicate unaffected nucleus. Scale bar = 100 µm.

In the 4HNE analysis, the immunomarker levels showed no significant differences compared to the positive and negative controls. With the exception of L350, which maintained the levels of the positive control.

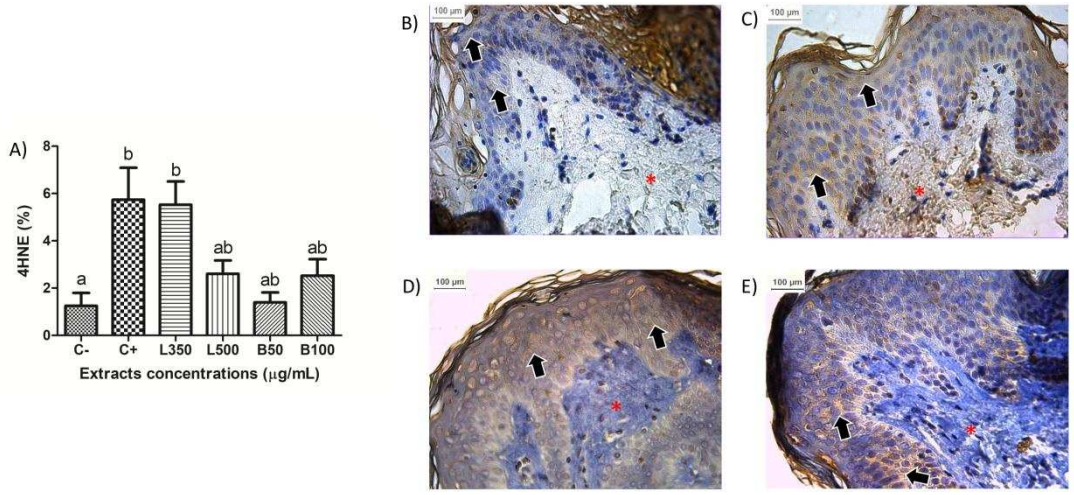

Figure 8. (A) Proportion of 4HNE evidenced by immunostaining in ex vivo skin fragments exposed to methylglyoxal and treated with leaf and bark extracts of *Commiphora leptophloeos.* (B, C and D) Representative photomicrograph of 4HNE immunostaining of skin C-: skin fragments not exposed to methylglyoxal (culture medium only); C+: skin fragments exposed to methylglyoxal at a concentration of 650 µM; L350, L500, B50, and B100: tissues exposed to methylglyoxal and treated with leaf (350 and 500 µg/mL) and bark extracts (50, and 100 µg/mL) of *Commiphora leptophloeos*. According to the Tukey test, groups with different letters exhibit statistically significant differences ($p<0.05$). Photomicrograph of epithelial tissue with immunohistochemical staining for 4HNE and hematoxylin staining. Control group = Skin fragments not exposed to methylglyoxal (B), skin fragments exposed to methylglyoxal at concentrations of 650 µM (C), skin fragments exposed to methylglyoxal and treated with leaf extract at 350 µg/mL (D), skin fragments exposed to methylglyoxal and treated with bark extract at 100 µg/mL (E). Black arrows indicate immunohistochemical signal for 4HNE in the epidermis. Red asterisks indicate dermis. Scale bar = 100 µm.

2.4.4. RNA Extraction and Quantitative Reverse Transcription PCR (RT-qPCR)

Considering the real-time qPCR results, we can observe a downregulation of TLR-4 at B100 and of NFk-B and COX-2 expression at L500 and B100 concentrations (figure 9 A, B and C). In figure 9 D and E, we observe the upregulation of the NRF-2 and HO-1 gene expression at L500.

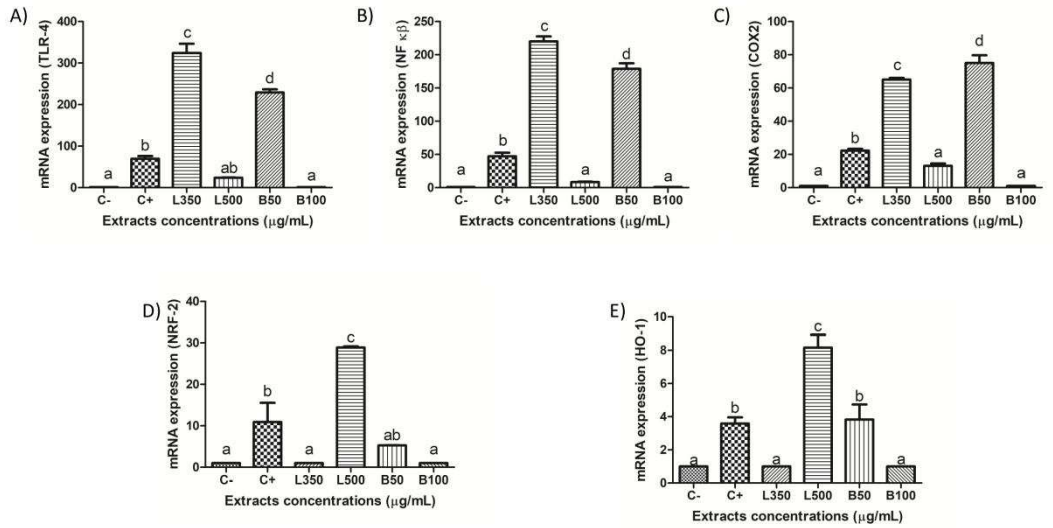

Figure 9. Gene amplification by real-time PCR. Expression of the TLR-4 gene (A); Expression of NFk-B (B); Expression of COX-2 (C); Expression of NRF-2 (D); Expression of HO-1 (E). C-: skin fragments not exposed to methylglyoxal (culture medium only); C+: skin fragments exposed to methylglyoxal at a concentration of 650 µM; L350, L500, B50, and B100: tissues exposed to methylglyoxal and treated with leaf (350 and 500µg/mL) and bark extracts (50, and 100 µg/mL) of *Commiphora leptophloeos*.. According to the Tukey test, groups indicated with different letters exhibit statistically significant differences ($p<0.05$).

2.4.5. Skin Permeation

The permeation study through a biological barrier was conducted to evaluate the penetration potential of *Commiphora leptophloeos* leaf and bark extracts across the skin, as well as their retention in the different skin layers. The levels of L350, L500, B50, and B100 found in the skin layers and the receptor solution after 24 hours are illustrated in Table 2 and Figure 10. From the total amount of L350 applied to the skin, a concentration of 48,12% was found in the receptor solution (RS), 0,09% was quantified in the stratum corneum (SC) layer, and 0,03% in the epidermis (EP). Approximately a concentration of 0,12% was observed in the dermis (DE). From the total amount of L500 applied to the skin, a concentration of 35,86% was found in the receptor solution (RS), 0,002% was quantified in the stratum corneum (SC) layer, and 0,001% in the epidermis (EP). Approximately a concentration of 0,003% was observed in the dermis (DE). From the total amount of B50 applied to the skin, a concentration of 0,53% was found in the receptor solution (RS), 11,95% was quantified in the

stratum corneum (SC) layer, and 1,29% in the epidermis (EP). Approximately a concentration of 7,68% was observed in the dermis (DE). From the total amount of B100 applied to the skin, a concentration of 0,09% was found in the receptor solution (RS), 2,90% was quantified in the stratum corneum (SC) layer, and 0,01% in the epidermis (EP). Approximately a concentration of 0,09% was observed in the dermis (DE).

The analytical curves used showed a satisfactory linear relationship, with linear equations for bark extract: $y = 11.792x - 0.0002$ in PBS (0.006-0.060 μg mL^{-1}, $R^2 = 0.9988$) and $y = 0.6452x + 0.0232$ in acetonitrile (0.300-1.000 μg mL^{-1}, $R^2 = 0.9976$). Similarly, a satisfactory linear relationship was observed for the leaf extract with the equation: $y = 0.2536x + 0.035$ in PBS (0.020-0.700 μg mL^{-1}, $R^2 = 0.9649$) and $y = 47.907x - 0.1251$ in acetonitrile (0.006-0.020 μg mL^{-1}, $R^2 = 0.9955$).

Table 2. Concentration of extracts found in the skin layers and receptor solution.

Bark					
	Initial	**Stratum corneum**	**Epidermis**	**Dermis**	**Receiving solution**
μg/mL	50,00	5,97 ± 0,88	0,64 ± 0,06	3,84 ± 1,39	0,26 ± 0,004
%	100	11,95 ± 1,77	1,29 ± 0,12	7,68 ± 2,78	0,53 ± 0,01
μg/mL	100,00	2,90 ± 1,02	0,01 ± 0,06	2,94 ± 1,41	0,09 ± 0,002
%	100	2,90 ± 1,02	0,01 ± 0,06	2,94 ± 1,41	0,09 ± 0,002
Leaf					
	Initial	**Stratum corneum**	**Epidermis**	**Dermis**	**Receiving solution**
μg/mL	350,00	0,30 ± 0,07	0,10 ± 0,04	0,42 ± 0,14	168,40 ± 11,22

%	100	0,09 ± 0,02	0,03 ± 0,01	0,12 ± 0,04	48,12 ± 3,21
µg/mL	500,00	0,010 ± 0,005	0,004 ± 0,01	0,018 ± 0,02	146,81 ± 41,17
%	100	0,002 ± 0,001	0,001 ± 0,001	0,004 ± 0,003	35,86 ± 8,23

The percentages of skin permeation of the leaf and bark extracts of *Commiphora leptophloeos* is presented in Figure 10

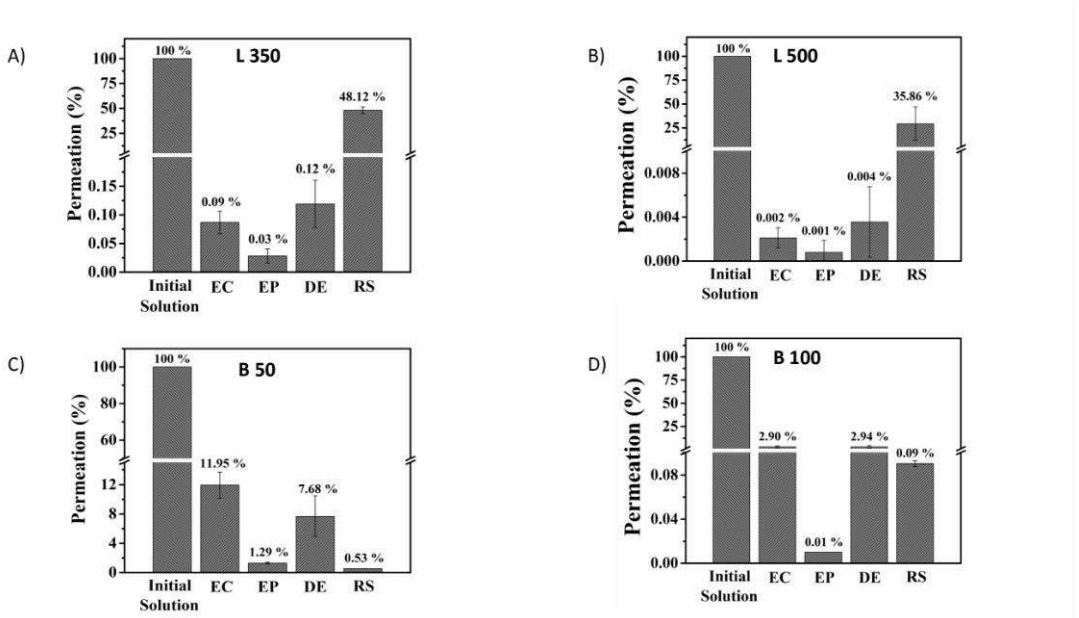

Figure 10. Cutaneous permeation levels of *Commiphora leptophloeos* leaf extracts at concentrations of 350 and 500 µg/mL (A and B) and bark extracts at concentrations of 50 and 100 µg/mL (C and D). EC - stratum corneum; EP - epidermis; DE - dermis; SR - receptor solution.

2.5. Discussion

Commiphora leptophloeos contains bioactive compounds widely used in traditional medicine, such as gallic acid, protocatechuic acid, and chlorogenic acid, which are known for their

antioxidant, anti-inflammatory, antiproliferative, and antimicrobial properties (De Souza Pereira et al., 2017). Based on this information, our group developed, for the first time, an *ex vivo* study using the aforementioned extracts to investigate these properties and assess whether they could protect the skin from external stressors.

Considering the ability of methylglyoxal to induce oxidative stress (Sugiura et al., 2021), we evaluated how stressed tissue, treated with *Commiphora leptophloeos* extracts, affected the activity of antioxidant enzymes and the expression of oxidative stress markers, such as the activity of SOD, CAT, and glutathione S-transferase (GST), as well as the presence of carbonylated proteins.

We observed that SOD, CAT, and GST activities increased upon exposure to MG (positive control). This increase in antioxidant enzymes induced by methylglyoxal has also been reported in other studies using human skin fibroblast and epithelial cell cultures and macrophages (Sejersen & Rattan, 2009; Costa et al., 2025), supporting the notion that the compound is capable of inducing continuous oxidative stress in the experimental model used.

On the other hand, a reduction in SOD and CAT activity was detected at B50 and B100 bark extract concentrations compared to the positive control, while GST activity for these extracts was increased. The decrease in SOD and CAT activity accompanied by an increase in GST at B50 and B100 concentrations suggests a selective antioxidant response, favoring the glutathione pathway. Plant extracts rich in phenolic compounds and terpenes, such as those from *C. leptophloeos* (Cordeiro et al., 2021; Muzykiewicz-Szymańska et al., 2024), have been described as modulators that primarily stimulate the expression of genes related to glutathione synthesis (Ma, 2013), which would explain this increase at the expense of other enzymes. Additionally, *C. leptophloeos* has shown superoxide radical scavenging activity (Cordeiro et al., 2021), which may also account for the differences observed among the antioxidant enzymes.

Conversely, the 350 µg/mL concentration of the leaf extract (L350) increased SOD and CAT activity levels beyond the positive control. This suggests that, at this concentration, the extract may not be capable of effectively scavenging superoxide radicals, resulting in increased enzyme activity to neutralize the excess free radicals induced by methylglyoxal.

GST activity levels did not show significant differences compared to the positive control in the L350 and L500 treatments; however, higher enzymatic activity was observed in the B50 and B100 treatments.

Regarding the damage marker, a higher amount of carbonylated protein was detected in the positive control, reaffirming the ability of methylglyoxal to induce oxidative damage to the tissue — as expected, since it generates advanced glycation end products (AGEs) and promotes the formation of reactive oxygen species (ROS), leading to protein oxidation (Wattanapitayakul et al., 2023).

On the other hand, all tested compounds were effective against protein carbonylation, maintaining levels similar to those of the negative control. This result, combined with the antioxidant enzyme data, suggests that the extracts were able to prevent oxidative damage, possibly through different mechanisms.

Plants contain intermediate metabolites capable of acting intracellularly to maintain homeostasis and protect cells against damage caused by various factors (Hussain et al., 2016). Previous studies have identified phenolic compounds in *Commiphora leptophloeos* whose molecular targets are associated with antioxidant defense and inflammatory responses. In addition to these compounds, flavonoids such as rutin have also been reported in this species (Cordeiro et al., 2021). Rutin is widely recognized for its broad biological activity, notably its antioxidant, anti-inflammatory, and cytoprotective properties (Ghorbani, 2017).

To investigate the potential of our extracts in protecting cells against oxidative stress and excessive inflammation, we selected, for PCR analysis, inflammatory mediators including **TLR-4**, **NF-κB**, and **COX-2**, as well as antioxidant mediators such as **NRF2** and **HO-1**.

As highlighted by Ferrara et al. (2021), methylglyoxal (MGO), through its stress-inducing capability, activates transcription factors related to cellular survival, such as nuclear factor erythroid 2–related factor 2 (NRF2). NRF2 plays a central role in the rapid cellular response to oxidative stress by upregulating the expression of endogenous antioxidant defenses (Johnson et al., 2008). Under homeostatic conditions, NRF2 remains inactive; however, under stress, it translocates to the nucleus and activates the transcription of antioxidant response elements (AREs), leading to the induction of a wide array of protective proteins, antioxidant enzymes, and factors that enhance cellular metabolism, thereby promoting the elimination of

reactive species and toxic metabolites that threaten cellular homeostasis (Cichon & Brown, 2014; Ying et al., 2024).

Toll-like receptors (TLRs) are transmembrane proteins that function as pattern recognition receptors (PRRs), primarily recognizing pathogen-associated molecular patterns (PAMPs), and are essential components of the innate immune response (Kawai & Akira, 2010). There is a well-established interaction between TLR-4 and the NF-κB signaling pathway. Upon PAMP recognition, TLR-4 triggers a cascade of intracellular events that culminate in NF-κB activation, resulting in the production of pro-inflammatory cytokines (Babu et al., 2024) and induction of **cyclooxygenase-2** (COX-2), which synthesizes prostaglandins — key inflammatory mediators (Liu et al., 2017). This relationship is reflected in our results, where all extract concentrations showing elevated TLR-4 expression also demonstrated increased levels of NF-κB and COX-2.

There is also a well-documented crosstalk between NRF2 and NF-κB pathways, in which NRF2 negatively regulates NF-κB activity. In other words, higher NRF2 expression is generally associated with reduced NF-κB activation (Ahmed et al., 2017). Furthermore, the NRF2 pathway is closely linked to the expression of heme oxygenase-1 (HO-1), as NRF2 directly induces the expression of this cytoprotective enzyme. Our findings support this regulatory relationship: the L500 extract, which showed the highest NRF2 expression levels, also exhibited lower expression of pro-inflammatory mediators and elevated HO-1 expression. Conversely, the L350 extract, which showed the highest permeation among all tested concentrations, had lower NRF2 expression and higher levels of pro-inflammatory markers, along with reduced HO-1 expression. This inverse regulatory pattern was also evident in the positive control group, further supporting the interplay between these molecular pathways.

Mast cells are well-characterized immune effector cells, primarily recognized for their roles in host defense against pathogens, modulation of both innate and adaptive immune responses, allergic reactions, and toxin neutralization (DeBruin et al., 2014). Due to their ability to release a broad spectrum of pro-inflammatory cytokines, an increased presence of mast cells is commonly observed at sites of inflammation (Theoharides et al., 2012).

In the present study, we did not observe a significant increase in mast cell numbers across any of the tested extract concentrations, including the positive control group. Regarding the treatments, the low number of mast cells observed in the extract-treated groups is likely

associated with the well-documented anti-inflammatory properties of *Commiphora leptophloeos* (De Souza Pereira et al., 2017).

Interestingly, the unexpectedly low mast cell counts in the positive control group may be attributed to the ability of advanced glycation end-products (AGEs), such as methylglyoxal (MGO), to rapidly trigger mast cell degranulation (Sick et al., 2010). This rapid release of granule contents could result in a transient presence of intact mast cells, thereby making their quantification less apparent under our experimental conditions.

Angiogenesis is a critical physiological process responsible for preserving microvascular integrity and, consequently, maintaining tissue homeostasis. This process is tightly regulated by a range of growth factors, and any reduction in their availability can significantly impair angiogenic activity (Bentov & Reed, 2015).

Among these factors, transforming growth factor-beta (TGF-β) and its co-receptor endoglin, play central roles by stimulating endothelial cell proliferation and migration—key events for the stabilization and survival of blood vessels. Elevated expression of endoglin in inflamed tissues is widely recognized as a marker of endothelial repair responses, facilitating neovascularization as a compensatory mechanism to preserve tissue viability (Russell et al., 2015).

As previously demonstrated, methylglyoxal induces oxidative stress (Desai et al., 2010), and it is well established that oxidative stress and inflammation can engage in a self-amplifying loop, leading to a state of “oxi-inflammation” (Valacchi et al., 2018). This interplay likely accounts for the elevated vascular density observed in the positive control group. In contrast, tissue samples treated with *Commiphora leptophloeos* extracts exhibited a marked reduction in blood vessel formation, maintaining levels comparable to the negative control. These findings suggest a potent anti-inflammatory effect of the extracts, capable of attenuating the inflammatory angiogenic response.

According to Sugiura et al. (2021), the constant presence of methylglyoxal (MG) in the skin can lead to the formation of advanced glycation end-products (AGEs) in collagen. The accumulation of carbonylated collagen, according to the authors, can result in skin aging, fibroblast apoptosis, and increased stiffness due to the reduction in elasticity. Collagen fibers are essential structural components of the extracellular matrix (ECM) in connective tissues, providing tensile strength and contributing to biomechanical resilience—functions primarily

attributed to type I collagen. Type III collagen, on the other hand, plays a crucial role in tissue repair and remodeling during the healing process (López De Padilla et al., 2021). Type I collagen is the most abundant protein in the human dermis, organizing with other fibrillar collagens, such as types III and V, to form bundles of mature and resilient fibers. These collagen structures are actively synthesized and organized by dermal fibroblasts, being fundamental for the integrity and mechanical homeostasis of the skin. However, oxidative stress induces irreversible dysfunctions in fibroblasts, representing one of the main factors associated with skin aging. Under stress conditions, collagen fragmentation increases, while collagen biosynthesis by fibroblasts is reduced (Fisher et al., 2008). Alterations in the fibroblast microenvironment impair their mechanical tension, which can lead to fibroblast inactivation or apoptosis, further exacerbating ECM degradation. This process is often accompanied by increased collagenase activity, which accelerates the breakdown of structural collagen fibers (Varani et al., 2006). It is noteworthy that the increased expression of type III collagen is a common marker in various human fibrotic diseases (Kuivaniemi et al., 2020). According to our results, the B50 and B100 concentrations led to an increase in type III collagen expression, suggesting a response to stress (Kuivaniemi et al., 2019).

As previously described, methylglyoxal (MG) acts as a critical intermediate in the formation of Advanced Glycation End Products (AGEs). The interaction of collagen with these AGEs induces chemical modifications that lead to the formation of irreversible cross-links between collagen fibers. This process significantly compromises the structural integrity of the extracellular matrix, resulting in the deformation of fibers and the loss of their essential biomechanical properties (Chen et al., 2022). These effects explain the reduction in type I collagen levels observed across all tested concentrations, as the increase in cross-links negatively interferes with collagen synthesis and homeostasis. Our experiment lasted for seven days, which is why our group hypothesizes that low levels of type I collagen were observed even in treated samples, as this time may not have been sufficient for the recovery of the fibers.

We also performed immunohistochemistry analyses to evaluate and visualize the effects of methylglyoxal and the extracts of *C. leptophloeos* in our experimental model, focusing on the analysis of filaggrin, catalase, 8 OHdG e 4 HNE. Filaggrin is a crucial protein for skin health, playing a key role in corneocyte formation and producing metabolites that assist in epidermal hydration and protection (Thyssen et al., 2014). Filaggrin levels can be reduced due to oxidative stress, and inflammation can lead to various consequences for the tissue, such as atopic dermatitis and dryness (Howell et al., 2009). Our analyses support these findings, as we

observed a reduction in filaggrin immunoexpression in the positive control. Studies employing glyoxal in tissue engineered in vitro models have also reported such a reduction, that was reduced following the administration of the anti-glycation compound (Cadau et al, 2015). Intriguingly, we also detected an even pronounced decrease in immunostaining at the different treatments with the extracts. Ex vivo human skin explant models have emerged as valuable tools for investigating biologia mecanisms and assessing the effects of bioactive compounds in a setting that closely mimic human physiological conditions (Neil et al., 2022). However, this model presents inherent limitations that may explain the reduction in filaggrin levels observed in our study following extracts treatment. It is estimated that the epidermis turns over every 40-56 days in humans (Koster, 2009). Moreover, an ex vivo human skin study demonstrated that filaggrin recovery in the epithelial tissue required approximately 10 days post injury (Rakita et al, 2020). These findings suggest that the restoration of structural and differentiation related protein involvedes time dependent processes, including active synthesis and cellular proliferation and differentiation, which may be compromised in explant cultures. Furthermore, given that our experimental protocol lasted 7 days, it is possible that there was insufficient time for filaggrin to be structurally reestablished following exposure to methylglyoxal and subsequent treatment with the extracts.

We also analyzed the potential of the extracts to prevent DNA damage in the cells by immunohistocchemistry. To this purpose, we used a well-established marker for oxidative damage to DNA, the 8-hydroxy-2-deoxyguanosine (8-OHdG). This marker is an oxidized derivative of guanosine and is widely recognized as a sensitive biomarker for oxidative stress-induced genotoxicity (Shekaftik & Nasirzadeh, 2021; Kim et al., 2010). Our findings revealed that treatment with the extracts at all tested concentrations significantly reduced nuclear immunostaining levels associated with DNA damage, except for L350. This protective effect was especially prominent at the highest concentrations from each extract group, L500 and B100. We attribute these results to the known antioxidant properties of *Commiphora leptophloeos* (Cordeiro et al., 2021), which likely enhance cellular defense mechanisms in a dose-dependent manner, possibly by supporting endogenous systems such as the glyoxalase pathway (Seo et al., 2014). This dose-responsiveness may explain the greater efficacy observed at elevated extract concentrations.

Methylglyoxal (MGO) is recognized as a key initiator of metabolic disturbances that can lead to the peroxidation of membrane lipids, a process strongly associated with oxidative damage (Dmitriev & Titov, 2009) which in turn, results in reactive carbonyl species (RCS), such as 4-

hydroxy-2-nonenal (4HNE), which can bind to and modify almost all types of proteins (Moldogazieva et al., 2023). The accumulation of 4HNE in the body can lead to cell death and various diseases, such as cardiovascular disorders, cancer, diabetes, Alzheimer's, and Parkinson's (Kiyuna et al., 2023; Lou et al., 2020). This mechanism likely accounts for the elevated levels of the lipid peroxidation marker 4-HNE, observed in the positive control group. At the L350 concentration, 4-HNE levels were comparable to those in the positive control, suggesting that at this dose, the leaf extract failed to effectively activate cellular defense mechanisms, such as the glyoxalase system, which is crucial for MGO detoxification (Honek, 2015). At the other concentrations, the extracts did not show statistically significant changes compared to either control. This suggests that, under the experimental conditions used, the extract did not exert a clear protective or harmful effect. Subtle or transient effects may have occurred, indicating the need for further studies focusing on this marker.

Interestingly, an inverse trend was observed for the bark extracts: the lower concentration proved more effective in mitigating lipid peroxidation. This may be explained by the PCR analysis, previously discussed, of the B100 condition, in which no expression of oxidative stress- or inflammation-related genes was detected, suggesting an alternative mechanism of action or efficient baseline suppression of cellular stress responses at this dose.

Regarding the cutaneous permeation index of the extracts, it is well established that plants contain active compounds capable of penetrating the skin at varying concentrations, depending on their physicochemical properties and the delivery vehicle used (Muzykiewicz-Szymańska et al., 2024).

According to Nowak et al. (2021), greater accumulation of these substances in the deeper layers of the skin enhances their antioxidant efficacy. However, Bertges et al. (2020) suggest that, in certain contexts such as cosmetics, antioxidant activity on the skin surface is amplified when permeation into deeper layers is reduced.

Supporting this, our analyses showed that the concentrations with the lowest permeation—specifically L500 and B50, corresponding to the leaf and bark groups—exhibited higher expression levels of antioxidant defense genes (NRF-2 and HO-1). Conversely, the concentrations with the highest permeation (L350 and B100) demonstrated the opposite effect. Notably, the L350 concentration, which exhibited the greatest permeation among all tested extracts, yielded comparatively unsatisfactory results across the assays conducted in this study.

2.6. Conclusion

In this study, it was observed that the various extracts of *C. leptophloeos* exhibit multifaceted effects on human skin subjected to glycation-induced stress. The extracts demonstrated significant antioxidant properties, likely mediated by distinct mechanisms—particularly at the concentrations of L500, B50, and B100—as evidenced by oxidative stress assays. This antioxidant effect was further supported by the reduction in carbonylated protein detection across the tested extracts, as well as by the observed decrease in oxidative DNA damage through immunohistochemical analysis at the concentrations of L500, C50, and B100.

Moreover, the extracts exhibited anti-inflammatory potential, with the most pronounced effects seen at the higher concentrations of leaf and bark extracts (L500 and B100, respectively), as indicated by the downregulation of TLR-4, NF-κB, and COX-2—key genes in the inflammatory response. Although mast cell quantification did not mirror this trend, it is important to consider that molecular and biochemical changes often precede morphological alterations, which may not yet be apparent in histological analyses.

In this context, the increased expression of Nrf2, along with elevated HO-1 levels at the F500 concentration, suggests the activation of protective cellular stress response pathways. Overall, among the tested extracts, the leaf extract at 500 μg/mL (L500) emerged as the most promising candidate, warranting further investigation into the protective effects of *C. leptophloeos* against oxidative and glycative skin damage.

2.7. References

AEBI, Hugo. Catalase in vitro. In: **Methods in enzymology**. Academic press, 1984. p. 121-126.

AHMED, Syed Minhaj Uddin et al. Nrf2 signaling pathway: Pivotal roles in inflammation. **Biochimica et Biophysica Acta (BBA)-Molecular basis of disease**, v. 1863, n. 2, p. 585-597, 2017.

BABU, Nagendra et al. TLR-4: a promising target for chemotherapy-induced peripheral neuropathy. **Molecular Biology Reports**, v. 51, n. 1, p. 1099, 2024.

Bentov, Itay; Reed, May J. The effect of aging on the cutaneous microvasculature. **Microvascular research**, v. 100, p. 25-31, 2015.

Bertges, F. S., Da Penha Henriques Do Amaral, M., Rodarte, M. P., Vieira Fonseca, M. J., Sousa, O. V., Pinto Vilela, F. M., et al. (2020). Assessment of chemical changes and skin penetration of green Arabica coffee beans biotransformed by Aspergillus oryzae. Biocatal. Agric. Biotechnol. 23, 101512. doi:10.1016/j.bcab.2020.101512.

BRESCIANI, Guilherme; DA CRUZ, Ivana Beatrice Mânica; GONZÁLEZ-GALLEGO, Javier. Manganese superoxide dismutase and oxidative stress modulation. Advances in clinical chemistry, v. 68, p. 87-130, 2015.

CADAU, Sébastien et al. In vitro glycation of an endothelialized and innervated tissue-engineered skin to screen anti-AGE molecules. **Biomaterials**, v. 51, p. 216-225, 2015.

Chen CY, Zhang JQ, Li L, Guo MM, He YF, Dong YM, Meng H, Yi F. Advanced Glycation End Products in the Skin: Molecular Mechanisms, Methods of Measurement, and Inhibitory Pathways. Front Med (Lausanne). 2022 May 11;9:837222. doi: 10.3389/fmed.2022.837222. PMID: 35646963; PMCID: PMC9131003.

CHIARELLO, Delia I. et al. Cellular mechanisms linking to outdoor and indoor air pollution damage during pregnancy. **Frontiers in endocrinology**, v. 14, p. 1084986, 2023.

CHURUKIAN CJ, SCHENK EA. A Toluidine Blue Method for Demonstrating Mast Cells. J Histotechnol. 1981;4: 85–86. doi:10.1179/his.1981.4.2.85

CICHON, Ann-Christin; BROWN, David R. Nrf-2 regulation of prion protein expression is independent of oxidative stress. **Molecular and Cellular Neuroscience**, v. 63, p. 31-37, 2014.

CORDEIRO, Maria Lucia da Silva et al. Antioxidant activities of Commiphora leptophloeos (Mart.) JB Gillett)(Burseraceae) leaf extracts using in vitro and in vivo assays. **Oxidative Medicine and Cellular Longevity**, v. 2021, n. 1, p. 3043720, 2021.

Costa, E.P., Santos, M.M., Paula, R.A., Silva, D.A., Lopes, R.P., Teixeira, R.R., Gonçalves, R.V., 2025. Antioxidant and Anti-inflammatory Activity of Eugenol, Bis-eugenol, and Clove Essential Oil: An In Vitro Study. **ACS Omega,** Article ASAP**.** https://doi.org/10.1021/acsomega.5c04146

Cupertino MC, Costa KLC, Santos DCM, Novaes RD, Condessa SS, Neves AC, et al. Long-lasting morphofunctional remodelling of liver parenchyma and stroma after a single exposure to low and moderate doses of cadmium in rats. Int J Exp Pathol. 2013;94: 343–351. doi:10.1111/iep.12046.

DANTAS-MEDEIROS, Renato et al. Mass spectrometry characterization of Commiphora leptophloeos leaf extract and preclinical evaluation of toxicity and anti-inflammatory potential effect. Journal of Ethnopharmacology, v. 264, p. 113229, 2021.

DEBRUIN, Erin J. et al. Mast cells in human health and disease. **Mast Cells: Methods and Protocols**, p. 93-119, 2014.

DE MELO ALCÂNTARA, Lucas Felipe et al. Toxicological safety, antioxidant activity and phytochemical characterization of leaf and bark aqueous extracts of Commiphora leptophloeos (Mart.) JB Gillett. Journal of Toxicology and Environmental Health, Part A, v. 86, n. 16, p. 557-574, 2023.

DESAI, Kaushik M. et al. Oxidative stress and aging: is methylglyoxal the hidden enemy?. Canadian journal of physiology and pharmacology, v. 88, n. 3, p. 273-284, 2010.

DE SOUZA PEREIRA, Jorge J. et al. Commiphora leptophloeos phytochemical and antimicrobial characterization. Frontiers in microbiology, v. 8, p. 52, 2017.

DIETERICH S, BIELIGK U, BEULICH K, HASENFUSS G, PRESTLE J. Gene Expression of Antioxidative Enzymes in the Human Heart. Circulation. 2000;101: 33–39. doi:10.1161/01.CIR.101.1.33

DMITRIEV, L. F.; TITOV, V. N. Lipid peroxidation in relation to ageing and the role of endogenous aldehydes in diabetes and other age-related diseases. **Ageing Research Reviews**, v. 9, n. 2, p. 200-210, 2010.

ERSHOVA, O. A. et al. Oxidative stress and catalase gene. Bulletin of experimental biology and medicine, v. 161, n. 3, p. 400-403, 2016.

Ferrara, Francesca et al. Redox regulation of cutaneous inflammasome by ozone exposure. **Free Radical Biology and Medicine**, v. 152, p. 561-570, 2020.

Ferrara, Francesca et al. Inflammasome activation in pollution-induced skin conditions. Plastic and reconstructive surgery, v. 147, n. 1S-2, p. 15S-24S, 2021.

Fisher, Gary J.; Varani, James; Voorhees, John J. Looking older: fibroblast collapse and therapeutic implications. Archives of dermatology, v. 144, n. 5, p. 666-672, 2008.

FRAILE-RAMOS, Juan et al. Hepatic Oxi-Inflammation and Neophobia as Potential Liver–Brain Axis Targets for Alzheimer's Disease and Aging, with Strong Sensitivity to Sex, Isolation, and Obesity. **Cells**, v. 12, n. 11, p. 1517, 2023.

GHORBANI, Ahmad. Mechanisms of antidiabetic effects of flavonoid rutin. **Biomedicine & Pharmacotherapy**, v. 96, p. 305-312, 2017.

Gonçalves R V., Novaes RD, Matta SLP, Benevides GP, Faria FR, Pinto MVM. Comparative Study of the Effects of Gallium-Aluminum-Arsenide Laser Photobiomodulation and Healing Oil on Skin Wounds in Wistar Rats: A Histomorphometric Study. Photomed Laser Surg. 2010;28: 597–602. doi:10.1089/pho.2009.2669.

GUO, Min et al. Extracts of dracocephalum tanguticum maxim ameliorate acute alcoholic liver disease via regulating transcription factors in mice. Frontiers in Pharmacology, v. 13, p. 830532, 2022.

HABIG WH, PABST MJ, JAKOBY WB. Glutathione S-Transferases. J Biol Chem. 1974;249: 7130–7139. doi:10.1016/S0021-9258(19)42083-8

HONEK, John F. Glyoxalase biochemistry. **Biomolecular Concepts**, v. 6, n. 5-6, p. 401-414, 2015.

HOWELL, Michael D. et al. Cytokine modulation of atopic dermatitis filaggrin skin expression. **Journal of Allergy and Clinical Immunology**, v. 124, n. 3, p. R7-R12, 2009.

JOHNSON, Jeffrey A. et al. The Nrf2–ARE pathway: an indicator and modulator of oxidative stress in neurodegeneration. **Annals of the new York Academy of Sciences**, v. 1147, n. 1, p. 61-69, 2008.

KAWAI, Taro; AKIRA, Shizuo. The role of pattern-recognition receptors in innate immunity: update on Toll-like receptors. **Nature immunology**, v. 11, n. 5, p. 373-384, 2010.

KIM, Junghyun et al. Methylglyoxal induces cellular damage by increasing argpyrimidine accumulation and oxidative DNA damage in human lens epithelial cells. Biochemical and biophysical research communications, v. 391, n. 1, p. 346-351, 2010.

KIYUNA, Ligia A. et al. 4-Hydroxynonenal impairs miRNA maturation in heart failure via Dicer post-translational modification. **European heart journal**, v. 44, n. 44, p. 4696-4712, 2023.

KOSTER, Maranke I. Making an epidermis. **Annals of the New York Academy of Sciences**, v. 1170, n. 1, p. 7-10, 2009.

KUIVANIEMI, Helena; TROMP, Gerard. Type III collagen (COL3A1): Gene and protein structure, tissue distribution, and associated diseases. Gene, v. 707, p. 151-171, 2019.

LIU, Ting et al. NF-κB signaling in inflammation. **Signal transduction and targeted therapy**, v. 2, n. 1, p. 1-9, 2017.

López de Padilla, Consuelo M. et al. Picrosirius red staining: revisiting its application to the qualitative and quantitative assessment of collagen type I and type III in tendon. **Journal of Histochemistry & Cytochemistry**, v. 69, n. 10, p. 633-643, 2021.

LOU, Bowen. The increased concentration of 4-Hydroxynonenal in aldh3a1 zebrafish mutants disrupts pancreas development, leading to hyperglycaemia and retina hyaloid vasculature alteration. 2020. Tese de Doutorado.

Lowry, O.H.; Rosebrough, N.J.; Farr, A.L. Protein Measurement with the Folin Phenol Reagent. J. Biol. Chem. 1951, 193, 265–275.

LEVINE, R.L.; GARLAND, D.; OLIVER, C.N.; AMICI, A.; CLIMENT, I.; LENZ, A.G.; AHN, B.W.; SHALTIEL, S.; STADTMAN, E.R. Determination of Carbonyl Content in Oxidatively Modified Proteins. Methods Enzymol. 1990, 186, 464–478.

MA, Qiang. Role of nrf2 in oxidative stress and toxicity. **Annual review of pharmacology and toxicology**, v. 53, n. 1, p. 401-426, 2013.

MAJTAN, Juraj; BUCEKOVA, Marcela; JESENAK, Milos. Natural products and skin diseases. Molecules, v. 26, n. 15, p. 4489, 2021.

MOLDOGAZIEVA, Nurbubu T. et al. Lipid peroxidation: Reactive carbonyl species, protein/DNA adducts, and signaling switches in oxidative stress and cancer. Biochemical and Biophysical Research Communications, v. 687, p. 149167, 2023.

Morais-santos, Monica et al. Basal cells show increased expression of aromatase and estrogen receptor α in prostate epithelial lesions of male aging rats. Endocrinology, v. 159, n. 2, p. 723-732, 2018.

MUZYKIEWICZ-SZYMAŃSKA, Anna et al. Sanguisorba officinalis L. ethanolic extracts and essential oil–chemical composition, antioxidant potential, antibacterial activity, and ex vivo skin permeation study. **Frontiers in Pharmacology**, v. 15, p. 1390551, 2024.

Neil, MS Jessica E. et al. A new ex vivo skin model for mechanistic understanding of putative anti-inflammatory topical therapeutics. International Journal of Pharmaceutics, v. 617, p. 121610, 2022.

NOURIAN DEHKORDI, Azar et al. Skin tissue engineering: wound healing based on stem-cell-based therapeutic strategies. Stem cell research & therapy, v. 10, n. 1, p. 111, 2019.

Nowak, A., Cybulska, K., Makuch, E., Kucharski, Ł., Różewicka-Czabańska, M., Prowans, P., et al. (2021a). In vitro human skin penetration, antioxidant and antimicrobial activity of ethanol-water extract of fireweed (Epilobium angustifolium L.). Molecules 26, 329. doi:10.3390/molecules26020329.

OMARI SHEKAFTIK, Soqrat; NASIRZADEH, Nafiseh. 8-Hydroxy-2′-deoxyguanosine (8-OHdG) as a biomarker of oxidative DNA damage induced by occupational exposure to nanomaterials: A systematic review. **Nanotoxicology**, v. 15, n. 6, p. 850-864, 2021.

R. Dantas-Medeiros, A. C. Zanatta, L. B. F. C. de Souza, J. M. Fernandes, B. Amorim-Carmo, M. Torres-Rêgo, M. de F. Fernandes-Pedrosa, W. Vilegas, T. A. de S. Araújo, S. Michel, R. Grougnet, G. M. Chaves, S. M. Zucolotto. Antifungal and Antibiofilm Activities of B-Type Oligomeric Procyanidins From Commiphora Leptophloeos Used Alone or in Combination With Fluconazole Against Candida Spp. *Front Microbiol* 2021, *12*. https://doi.org/10.3389/fmicb.2021.613155.

RAKITA, Ana et al. Re-epithelialization and immune cell behaviour in an ex vivo human skin model. Scientific reports, v. 10, n. 1, p. 1, 2020.

Russell, Nicola S. et al. Blood and lymphatic microvessel damage in irradiated human skin: The role of TGF-β, endoglin and macrophages. Radiotherapy and Oncology, v. 116, n. 3, p. 455-461, 2015.

SARTORI, Adriano; BECHARA, Etelvino José Henriques. Metilglioxal: uma toxina endógena?. Química Nova, v. 33, p. 2193-2201, 2010.

SEJERSEN, Henrik; RATTAN, Suresh IS. Dicarbonyl-induced accelerated aging in vitro in human skin fibroblasts. **Biogerontology**, v. 10, n. 2, p. 203-211, 2009.

Seo, Kyuhwa et al. Resveratrol attenuates methylglyoxal-induced mitochondrial dysfunction and apoptosis by Sestrin2 induction. Toxicology and applied pharmacology, v. 280, n. 2, p. 314-322, 2014.

SHARMA, Anamika et al. Berberis lycium fruit extract and its phytoconstituents berberine and rutin mitigate collagen–CFA-induced arthritis (CIA) via improving GSK3β/STAT/Akt/MAPKs/NF-κB signaling axis mediated oxi-inflammation and joint articular damage in murine model. **Inflammopharmacology**, v. 30, n. 2, p. 655-666, 2022.

SICK, E. et al. Advanced glycation end products (AGEs) activate mast cells. British journal of pharmacology, v. 161, n. 2, p. 442-455, 2010.

SUGIURA, Ko et al. Carbonylation of skin collagen induced by reaction with methylglyoxal. Biochemical and Biophysical Research Communications, v. 562, p. 100-104, 2021.

T. de A. ANDRADE, J.R. de Jesus, M.V. de Sousa Pereira, P. de Tarso Garcia, M.A. Pimentel Falcão, C.I. Banderó Walker, L. Abrahão Frank, M. Russo Serafini, Successful preparation of a biopolymeric nanocarrier enables controlled release of antinociceptive monoterpene for local pain management after transdermal barrier permeation, J Appl Polym Sci 141 (2024). https://doi.org/10.1002/app.55568.

THEOHARIDES, Theoharis C. et al. Mast cells and inflammation. Biochimica et Biophysica Acta (BBA)-Molecular Basis of Disease, v. 1822, n. 1, p. 21-33, 2012.

T. HUSSAIN, B. Tan, Y. Yin, F. Blachier, M. C. B. Tossou, and N. Rahu, "Oxidative stress and inflammation: what polyphe-nols can do for us?," Oxidative Medicine and Cellular Longevity, vol. 2016, 9 pages, 2016.

THYSSEN, Jacob P.; KEZIC, Sanja. Causes of epidermal filaggrin reduction and their role in the pathogenesis of atopic dermatitis. Journal of Allergy and Clinical Immunology, v. 134, n. 4, p. 792-799, 2014.

Valacchi, Giuseppe et al. Redox regulation of inflammatory processes. 2016.

VALACCHI, G. et al. Ox-Inflammation: from subclinical condition to pathological biomarker. **Front. Physiol**. 9: e858. 2018.

Varani, James et al. Decreased collagen production in chronologically aged skin: roles of age-dependent alteration in fibroblast function and defective mechanical stimulation. The American journal of pathology, v. 168, n. 6, p. 1861-1868, 2006.

V. C. Da Silva, G. C. B. Guerra, D. F. D. S. Araújo, E. R. De Araújo, A. A. De Araújo, R. Dantas-Medeiros; A. C. Zanatta, I. L. G. Da Silva, R. F. De Araújo Júnior, D. Esposito, M. Moncada, S. M. Zucolotto. Chemopreventive and Immunomodulatory Effects of Phenolic-Rich Extract of Commiphora Leptophloeos against Inflammatory Bowel Disease: Preclinical Evidence. *J Ethnopharmacol* **2024**, *328*, 118025. https://doi.org/10.1016/j.jep.2024.118025.

WANG, Gang *et al*. Metformin prevents methylglyoxal-induced apoptosis by suppressing oxidative stress in vitro and in vivo. Cell Death & Disease, v. 13, n. 1, p. 29, 2022.

WATTANAPITAYAKUL, Suvara K. et al. Unripe Carica papaya fresh fruit Extract protects against methylglyoxal-mediated aging in human dermal skin fibroblasts. **Preventive Nutrition and Food Science**, v. 28, n. 3, p. 235, 2023.

YING, Mengchao et al. Nrf-2/HO-1 activation protects against oxidative stress and inflammation induced by metal welding fume UFPs in 16HBE cells. **Scientific Reports**, v. 14, n. 1, p. 24057, 202